Ecophysiological study of some freshwater red algae from southern Japan

南日本産淡水紅藻類数種の生理生態に関する研究

Jumpei Kozono

The United Graduate School of Agricultural Sciences

Kagoshima University

March 2020

This PhD. dissertation was based on the following articles published in the journals.

1. Kozono, J., Nishihara, G. N., Endo, H., Terada, R. 2018. Effect of temperature and PAR on photosynthesis of an endangered freshwater red alga, *Thorea okadae*, from Kagoshima, Japan. Phycologia 57 (6): 619–629. DOI: 10.2216/18-26.1 (Online: 21 Sep 2018; Issue: November 2018)
2. Kozono, J., Nishihara, G. N., Endo, H., Terada, R. 2020. Photosynthetic activity in two heteromorphic life-history stages of a freshwater red alga, *Thorea gaudichaudii* (Thoreales) from Japan, in response to an irradiance and temperature gradient. Phycological Research DOI: 10.1111/pre.12416 (Online: 17 December 2019)
3. Kozono, J., Nishihara, G. N., Endo, H., Terada, R. 2020. T The temperature and light responses on the photosynthesis of two freshwater red algae, *Virescentia helminthosa* and *Sheathia arcuata* (Batrachospermaceae) from Japan. Journal of Applied Phycology DOI: 10.1007/s10811-019-01967-7 (in press; accepted: 9 October 2019)

Related article

4. Terada, R., Shikada, S., Watanabe, Y., Nakazaki, Y., Matsumoto, K., Kozono, J., Saino, N., Nishihara, G. N. 2016. Effect of PAR and temperature on the photosynthesis of Japanese alga, *Ecklonia radicosa* (Laminariales), based on field and laboratory measurements. Phycologia 55 (2): 178–186. DOI: 10.2216/15-97.1 (Online: 22 February 2016; Issue: March 2016)
5. Borlongan, I. A., Matsumoto, K., Nakazaki, Y., Shimada, N., Kozono, J., Nishihara, G. N., Shimada, S., Watanabe, Y., Terada, R. 2018. Photosynthetic activity of two life history stages of *Costaria costata* (Laminariales, Phaeophyceae) in response to PAR and temperature gradient. Phycologia 57 (2): 159–168. DOI: 10.2216/17-70.1 (Online: 11 January 2018; Issue: March 2018)
6. 小園淳平，Gregory N. Nishihara，遠藤光，寺田竜太 2018．鹿児島県産淡水紅藻オキチモズク *Nemalionopsis tortuosa* の光合成における光阻害と低温の複合作用．藻類 66 (1): 1–6.（2018 年 3 月 10 日）
7. Borlongan, I. A., Maeno, Y., Kozono, J., Endo, H., Shimada, S., Nishihara, G. N., Terada, R. 2019. Photosynthetic performance of *Saccharina angustata* (Laminariales, Phaeophyceae) at the southern boundary of distribution in Japan. Phycologia 58 (3): 300-309. DOI: 10.1080/00318884.2019.1571355 (Online: 19 March 2019; Issue June 2019)
8. Terada, R., Nakashima, Y., Borlongan, I. A., Shimabukuro, H., Kozono, J., Endo, H., Shimada, S., Nishihara, G. N. 2020. Photosynthetic activity including the thermal- and chilling-light sensitivities of a temperate Japanese brown alga *Sargassum macrocarpum*. Phycological Research DOI: 10.1111/pre.12398 (Online: 16 July 2019)

Abstract

The temperature and light responses of photosynthesis in some freshwater red algae, *Thorea okadae* (*To*), *Thorea gaudichaudii* (*Tg*; Thoreaceae), *Virescentia helminthosa* (*Vh*) and *Sheathia arcuata* (*Sa*; Batrachospermaceae) that can be found in southern Japan were determined by a pulse amplitude modulation (PAM)-chlorophyll fluorometer and dissolved oxygen sensors. As for *T. gaudichaudii*, those in both macroscopic (MAC) and microscopic (MIC) life-history stages in the heteromorphic life history were determined. Net oxygenic photosynthesis–irradiance models of four species revealed that the response to the irradiance was different in species (saturation irradiance [E_k]: 55.2 for *To*; 26.6 [MAC] and 30.0 [MIC] for *Tg*; 18.8 for *Vh*, 17.7 μmol photons m^{-2} s^{-1} for *Sa*), and the latter three species were considered to be adapted to the low irradiance environment. A temperature–dependent model (8~40°C) of net photosynthesis and dark respiration for four species showed characteristic shingle-peak temperature responses, and the gross photosynthetic rate (GP_{max}), was highest at around 26 – 36°C (30.8°C for *To*; 32.1°C [MAC] and 35.7°C [MIC] for Tg; 26.4°C for *Vh*; and 30.3°C for *Sa*). The dark respiration rate exponentially increased in response to temperature. The maximum quantum yields (F_v/F_m) in the Photosystem II (PSII) for four species were dome-shaped with respect to temperature; however, it was generally stable at low temperatures (8–20°C) with the highest value of around 0.4 – 0.6 occurring at 18.4°C for *To*, 17.8°C [MAC] and 15.0°C [MIC] for *Tg*, 18.5°C for *Vh* and 20.9°C

for *Sa*, respectively. Continuous exposure (12 hours) to low (50 or 100 μmol photons m^{-2} s^{-1}) and high (1,000 μmol photons m^{-2} s^{-1}) irradiance at 12, 16 and 24°C for four species revealed greater declines in their effective quantum yield (Φ_{PSII}) in all species under high irradiance, signifying the influence chronic photoinhibition. Nevertheless, the F_v/F_m mostly recovered after a subsequent 12-h dim-light acclimation for *V. helminthosa* and *S. arcuata*, suggesting the potential of recovery from day-time chronic photoinhibition. Diurnal change of Φ_{PSII} and incident irradiance of the macroscopic stage of *T. gaudichaudii* under the filed measurement revealed the midday depression of Φ_{PSII}; however, there was little direct sunlight due to the shading by the trees and algae were occurring on the shaded locations in the freshwater spring. Given the results of four freshwater red algae can be regarded to be well adapted to a low irradiance environment but can also be a partly tolerable relatively high irradiance environment that enables them to occur on the canal floor with no shade. Nevertheless, shading by the surrounding riparian vegetation is beneficial for many freshwater algae especially these four species, and it is relevant when proposing strategies for conservation and restoration.

要旨

南日本に生育する淡水産紅藻類 4 種，チスジノリ *Thorea okadae*，シマチスジノリ *Thorea gaudichaudii*（チスジノリ科），アオカワモズク *Virescentia helminthosa*，チャイロカワモズク *Sheathia arcuata*（カワモズク科）の光合成における温度や光の応答について，パルス変調クロロフィル蛍光測定および溶存酸素センサーを用いて明らかにした。シマチスジノリについては，異形世代交代の生活史を構成する巨視的な配偶体世代と顕微鏡的な胞子体世代の両方について明らかにし，他の 3 種については巨視的な世代を明らかにした。純光合成速度による 4 種の光合成−光曲線は種によって異なり，飽和光量（E_k）はチスジノリで 55.2 µmol photons m^{-2} s^{-1}，シマチスジノリで 26.6（巨視的世代）と 30.0 µmol photons m^{-2} s^{-1}（微少世代），アオカワモズクで 18.8 µmol photons m^{-2} s^{-1}，チャイロカワモズクで 17.7 µmol photons m^{-2} s^{-1} となったことから，チスジノリを除く 3 種は低光量環境に適応していることが示唆された。純光合成速度と暗呼吸速度に基づく水温 8〜40°C の光合成温度曲線は，総光合成速度（GP_{max}）が 26〜36°C にピークを有する曲線となり，GP_{max} はチスジノリで 30.8°C，シマチスジノリで 2.1°C（巨視的世代）と 35.7°C（微少世代），アオカワモズクで 26.4°C，チャイロカワモズクで 30.3°C が最高値になった。一方，暗呼吸速度は水温の上昇に沿って増加した。4 種の光化学系 II（PSII）の最大量子収率（F_v/F_m）は水温によって変化したが，一般に低温（8〜20°C）で 0.4〜0.6 と高い値を示して安定し，チスジノリで 18.4°C，シマチスジノリで 17.8°C（巨視的世代）と 15.0°C（微少世代），アオカワモズクで 18.5°C，チャイロカワモズクで 20.9°C が最高値を示した。光と水温の複合的なストレス応答を明らかにするため，弱光（50 または 100 µmol photons m^{-2} s^{-1}）と強光（1,000 µmol photons m^{-2} s^{-1}）条件で 12 時間光暴露を 12°C，16°C，24°C で行った結果，4 種とも強光条件で PSII の実効量子収率（Φ_{PSII}）が大幅に低下し，慢性的な強光阻害が示唆された。しかし，光暴露後の 12 時間の薄光（dim-light）馴致の結果，アオカワモズクとチャイロカワモズクの F_v/F_m はほぼ初期値まで回復したことから，日中の慢性的な強光阻害からの回復力を有することが示唆された。シマチスジノリを生育地の自然環境下で藻体に照射される光量と Φ_{PSII} の経時変化を測定した結果，正中前後に Φ_{PSII} がやや低下したが，生育地を囲む樹木等によって直射光はほぼ遮られており，本種の生育地は日陰の環境で維持されていた。4 種は低光量環境に基本的によく適応していると考えられるが，チスジノリなど，種によっては強光環境にも部分的に耐性があり，日陰のない水路の底質等にも見られる要因と考えられた。しかし，水路や河川を囲む樹木類による日陰の環境は 4 種を含む多くの淡水紅藻にとって有効と考えられ，これらの生育環境の保全を考慮する際に重要であると考えられる。

1. Introduction

Riparian vegetation bordering a reach of a stream plays an important role in influencing light and temperature by creating shade (Seath and Hampbrook 1990; Giller and Malmqvist 1998); therefore, these shaded habitats for biological organisms in the stream or irrigation canal can be maintained by the presence of both underwater and riparian environments. In fact, incident irradiance in this shaded environment seems insufficient for higher aquatic plants that can photosynthesize optimally under direct sunlight; however, low irradiance adaptation appears to be common in some freshwater red algae of Compsopogonales, Batrachospermales and Thoreales (Necchi and Zucchi 2001; Necchi 2005; Kusakariba and Necchi 2009; Fujimoto *et al.* 2014; Terada *et al.* 2016), and it might be a strategy to occupy stable habitat without competition.

The freshwater red algae generally inhabit clean inland waters including small freshwater springs, irrigation canals, and streams; therefore, these species can be a bioindicator for clean water (Kumano 2002). Hence, the extinction or disappearance of freshwater red algae from the habitat suggests the degradation of clean water or its environment that was caused by more or less of the human activities (Kumano 2002; Higa 2018). In fact, of the species of Japanese freshwater red algae, 41 species including the species used in the present study have been listed as an endangered species in Japan by

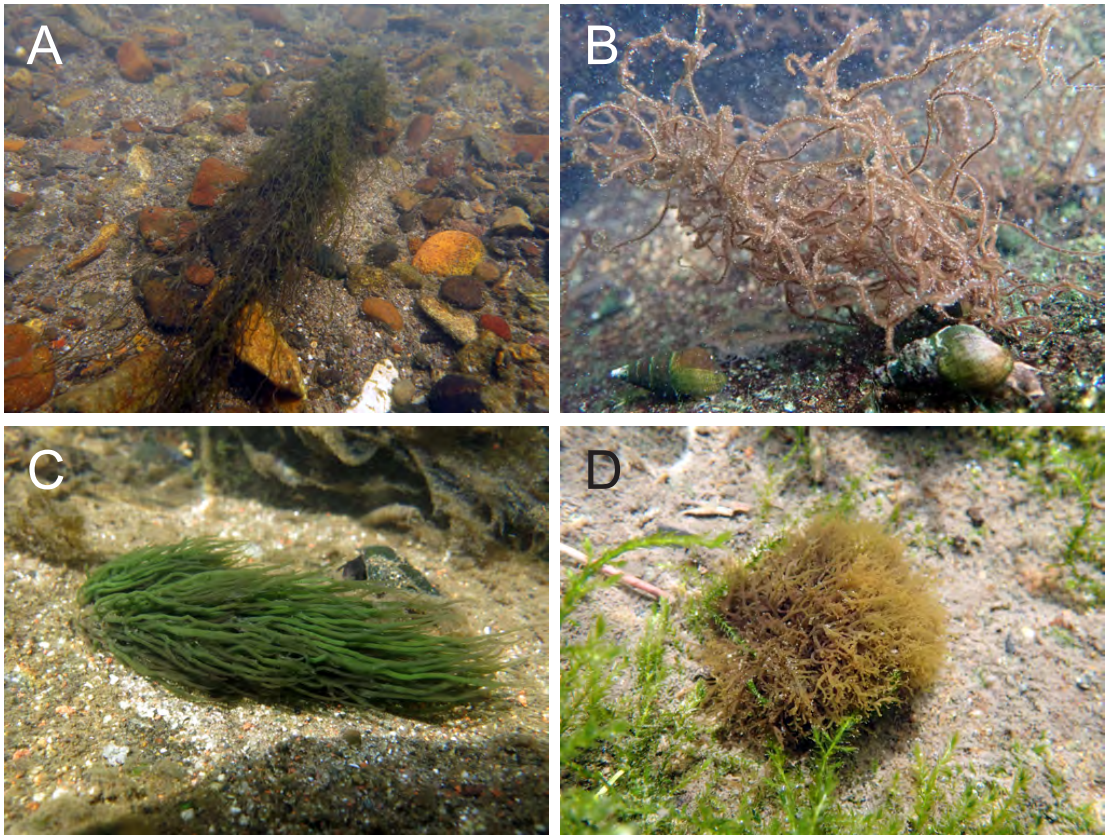

Fig. 1-1. Photos of algae showing the materials used in the present study. **A**: *Thorea okadae*, **B**: *Thorea gaudicahudii*, **C**: *Virescentia helminthos*a, **D**: *Sheathia arcuata*.

the Japanese Ministry of Environment (Red List, 4th edition revised in 2019, Japanese Ministry of Environment 2019).

Thorea okadae Yamada (Thoreaceae, Thoreales) was originally described by Yamada (1949) based on a specimen collected from Hishikari (Sendai-gawa River), Kagoshima Prefecture, Kyushu Island, Japan (Fig. 1-1A). This species can be found on pebbles and cobbles in creeks and rivers (Kumamo 2002; Higa *et al.* 2007), and is known as an endemic species in Japanese freshwaters that is distributed in the temperate regions

of Kyushu and Honshu Islands. However, confirmed habitats are quite limited, with less than 10 creeks and rivers in the whole of Japan (Seto *et al.* 1993). Furthermore, this alga was observed sparsely distributed only in the middle reaches of these bodies of water, indicating the high likelihood that local extinction of this taxon can occur due habitat degradation. In fact, this species is listed in the Red List as an endangered species by Japanese Ministry of Environment (Category: VU), and two sites of the habitat including its type locality at Hishikari, Sendai-gawa River, Kagoshima, have been registered as a natural monument of Japan since 1924 (Terada 2015b).

This species has a heteromorphic life history (Yoshizaki 1986; Kumano 2002) that alternates between a macroscopic life history stage (gametophyte) and a microscopic life history stage (sporophyte, known as *Chantransia*-phase). The macroscopic life history stage can generally be found on substrata during early winter through late spring (December through May). However, annual occurrence of this species in the type locality is unstable, and is periodically unobservable in its habitat, suggesting that biotic or abiotic factors influence the appearance of the species (Sabater *et al.* 2016).

A fundamental understanding of its life history, ecology, and physiology is essential toward the conservation of this species. Indeed, after the confirmation of sexual reproduction in the macroscopic gametophyte (Yoshizaki 1986; Necchi 1987), seasonal

changes in the two life-history stages, including the determination of the maturation period of this species, was reported from two sites; Kikuchi-gawa River in Kumamoto Prefecture, Kyushu Island and Yasumuro-gawa River in Hyogo Prefecture, Honshu Island (Higa *et al* 2007; Sato *et al.* 2013). However, despite past studies of its phenology (Higa *et al* 2007), ecophysiological processes, such as the response of photosynthesis along a gradient of temperature and irradiance remain to be examined in detail.

Thorea gaudichaudii C. Agardh (Thoreales) was reported from the tropical and subtropical regions of the western Pacific including the Philippines, Guam, Federated States of Micronesia and Japan (Fig. 1-1B: Agardh 1824; Kumano 2002; Necchi *et al*. 2015). This alga has also been listed as an endangered species in Japan by the Japanese Ministry of Environment (Category: CR+EN). In Japan, this species has been reported from the subtropical Ryukyu Archipelago (*i.e.*, Okinawa, Miyako, Hateruma and Yoron islands) and can be found in small freshwater springs (Seto 1979; Kumamo 2002; Suzawa *et al.* 2010; Terada *et al*. 2016c; Higa 2018). In fact, degradation of their habitat in relation to rural development and water pollution has been a serious concern in Okinawa; unfortunately, this species has disappeared from more than twenty sites due to these concerns (Terada 2015a; Terada *et al.* 2016c; Higa 2018).

In fact, conservation or restoration of its habitat is indispensable to avoid local

extinction at each island; however, it remains to be fully elucidated as to why its habitat is disappearing and what environmental factors are essential for their success. As this alga can be found in heavily shaded freshwater springs (Suzawa *et al.* 2010; Terada 2015a; Higa 2018), a recent study reported that the oxygenic photosynthesis–irradiance (*P–E*) curve of this alga quickly saturated under the low irradiance, suggesting that it is well adapted to the heavily shaded environment (Terada *et al*. 2016c). Given this finding, as a consequence of nearby land development, the subsequent loss of shade-providing vegetation near the habitat can the light environment and have an adverse effect on their population.

Low irradiance adaptation appears to be commonly found in some freshwater red algae of Thoreales (Necchi and Zucchi 2001; Necchi 2005; Fujimoto *et al*. 2014), and it might be a strategy to occupy the stable habitat without the competitors. However, our recent study focused only on the macroscopic stage of this alga that has a heteromorphic life history (Migita and Toma 1990); therefore, the knowledge of its ecophysiology for both life-history stages including the microscopic stage is essential for the better understanding its optimum environment. In fact, two species of marine red algae, *Pyropia tenera* (Kjellman) Kikuchi *et al*. and *Pyropia yezoensis* (Ueda) Hwang et Choi (Bangiales) that have heteromorphic life history are known to have different temperature

and irradiance optima of photosynthesis during its two life-history stages, and this difference is believed to be an adaptation strategy in relation to the irradiance and temperature environment of their respective occurrence period (Watanabe *et al*. 2014, 2016). Differences in the irradiance optima of photosynthesis in two heteromorphic life-history stages was also reported in some brown algae in Ectocarpales and Laminariales (*e.g.*, *Cladosiphon okamuranus* Tokida, *Cladosiphon umezakii* Ajisaka, *Alaria crassifolia* Kjellman, *Costaria costata* (C. Agardh) Saunders; Fukumoto *et al*. 2018, 2019; Borlongan *et al*. 2018, 2019), and the photosynthesis of microscopic stage is typically saturated at relatively low irradiance with a correspond low value of maximum photosynthesis, which is unlike values observed during the macroscopic stage.

On the one hand, in some marine algae including, *Kappaphycus alvarezii* (Doty) Doty ex Silva (Gigartinales) and *Sargassum patens* C. Agardh (Fucales), incident irradiance at noon under the direct sunlight is reported to cause the depression of photosystem II (*PSII*) photochemical efficiency, suggesting the occurrence of photoinhibition and/or photoadaptation under natural conditions (Kokubu *et al*. 2015; Terada *et al*. 2016a, b, 2018) with a Diving-PAM (Heinz Walz GmbH, Effeltrich, Germany); however, those in *T. gaudichaudii* remain to be elucidated.

Two species of a family Batrachospermaceae (Batrachospermales), *Virescentia*

helminthosa (Bory) Necchi, Agostinho et Vis (Fig. 1-1C; = *Batrachospermum helminthosum* Bory) and *Sheathia arcuata* (Kylin) Salomaki et Vis (Fig. 1-1D; = *Batrachospermum arcuatum* Kylin), which are known as "*Kawa-Mozuku* (river slimy algae)" in Japanese, are known to be distributed in temperate and subtropical regions of Japan and can be found at small streams and irrigation canals in the rural countryside (Kumano 2002); however, these species have been listed as an endangered species in Japan by the Japanese Ministry of Environment (Category: NT). Indeed, degradation of their habitats in relation to rural development and water pollution has been a serious concern; therefore, conservation and restoration of their habitats are indispensable to avoid local extinction for two species. However, it remains to be fully elucidated as to why its habitat is disappearing and what environmental factors are essential for their success. As these two species can be commonly found in shaded streams and irrigation canal, these two species seem to be well adapted to the low irradiance environment (Kumano 2002). Given this finding, and as a consequence of nearby land development, the subsequent loss of shade-providing riparian vegetation near the habitat can negatively affect the light environment and have an adverse effect on their populations.

Therefore, the ecophysiological information for these two species is essential for the better understanding their optimum environments. In fact, recent studies of two

freshwater red algae, *Nemalionopsis tortuosa* Yoneda et Yagi (Thoreales) and *T. gaudichaudii* revealed that these two species typically saturated at relatively low irradiance with a corresponding low value of maximum oxygenic photosynthesis (Fujimoto *et al.* 2014; Terada *et al*. 2016). Likewise, adaptation to a low irradiance environment was widely reported from the freshwater red algae of Brazil including *Compsopogon* (Compsopogonales), *Batrachospermum* (Batrachospermales) and *Thorea* (Necchi and Zucchi 2001; Necchi 2005; Kusakariba and Necchi 2009). Nevertheless, the knowledge of ecophysiology for *V. helminthosa* and *S. arcuata* from Japan remains to be elucidated.

In the present study, we focused on revealing the effect of temperature and irradiance on photosynthesis, as well as low irradiance adaptation of four freshwater red algae species, *T. okadae*, *T. gaudichaudii*, *V. helminthosa* and *S. arcuata* from Kagoshima, Japan. We hypothesized that there was a low requirement for irradiance in the two species, since they found in well-shaded environments in streams and irrigation canals. We also examined the hypothesis that photosystem II (*PSII*) photochemical efficiency was sensitive to irradiance by using the pulse amplitude modulation-chlorophyll (PAM) fluorometry, and examined the possibility of the occurrence for chronic photoinhibition. We expect that this study will help to advance conservation and restoration activities of

these two endangered species.

2. Materials and methods

2.1. Sample collection and stock maintenance

2.1.1. *T. okadae*

Field surveys were conducted at a Sendai-gawa River (32°0’51” N 130°36’57” E) in Hishikari, Isa City, Kagoshima Prefecture, Japan. During the monitoring period from 8 – 9 August 2015, and from 29 December 2015 through 4 January 2016, we deployed a temperature data logger (UA-002-64 HOBO; Onset Computer Co., USA) in the *T. okadae* population of the river bed and recorded water temperature every 30 minute. A submersible irradiance data logger (DEFI-L; JFE Advantech Co., Ltd., Japan) was also used to record underwater irradiance in the habitat at the same depth of *T. okadae* individuals (0.5–0.8 m deep). Irradiance was measured at 1 Hz, and one-minute averages were then calculated in the laboratory. During the duration of underwater irradiance measurement, surface irradiance without shading was also measured adjacent to the freshwater spring using the same model of data logger. It is relevant to note that the site experienced fine clear skies during the period of measurements.

The samples for laboratory experiments were collected at the same study site of

the irradiance and temperature measurements. Specimens for oxygen production and PAM fluorometry measurements were collected on 27 April 2015; while those for photoinhibition–recovery experiments were collected on 25 December 2015 and 4 February 2016. More than ten individuals were collected and stored in 500 mL plastic bottles with the freshwater from the study site. Bottles were stored in a cooler at approximately the same temperature as the study site, and were transported to the laboratory. The samples were maintained for one to three days before each experiment in 500 mL flasks at 16°C, which is approximately the same water temperature as that of sampling site on the sampling date. The flasks were filled with sterilized freshwater that was collected from the freshwater spring near the study site. The irradiance during the maintenance incubations was 90 μmol photons m^{-2} s^{-1} (12:12 hours light: dark cycle; MTI-201B incubator, ELYA, Tokyo Rikakikai Co., Ltd., Tokyo, Japan).

2.1.2. *T. gaudichaudii*

The samples of *T. gaudichaudii* for laboratory experiments were collected at the freshwater springs locally known as "*Injiago*" (0.4–0.5 m deep) in Yoron-jima island (27°01'48.5"N 128°26'21.5"E) on 30 November 2016 for the microscopic stage measurement and "*Ufukubuga*" (0.2–0.4 m deep) in Okinawa-jima island (26°28'55.9"N

127°59'09.8"E) on 30 January and 24 February 2018 for the macroscopic stage measurement, respectively. Additional samples were also collected at *Injiago* on 18 March 2018 for the macroscopic stage measurement to confirm the reproducibility of results. We note that the sample collection in Yoron-jima was the same as a previous report (Terada *et al*. 2016c).

Samples were collected in a manner to avoid influencing the abundance of the natural population; therefore, we minimized the number of specimens collected for each experiment. Approximately twenty individuals (or entangled masses for the microscopic stage) for each life-history stage were collected and stored in 500 mL polycarbonate bottles with the freshwater from the study site. Bottles were stored in a cooler at approximately the same temperature as the study site, and were transported to the laboratory. The samples were maintained for one to three days before each experiment in 500 mL flasks at 20°C, which is approximately the same water temperature as that of sampling site on the sampling date. The flasks were filled with sterilized freshwater that was collected from the freshwater spring near the study site. The irradiance during the maintenance incubations was 50 μmol photons m^{-2} s^{-1} (12:12 h light: dark cycle; MTI-201B incubator, ELYA, Tokyo Rikakikai Co., Ltd., Tokyo, Japan).

2.1.3. *V. helminthosa* and *S. arcuata*

The samples of *V. helminthosa* was collected at an irrigation canal at Katsume (0.2–0.3 m deep; 31°22'10.9"N 130°21'16.3"E) in Minami-Kyushu City, Kagoshima Prefecture, Kyushu Island, Japan on 18 April 2015 (for the experiment of oxygenic photosynthesis) and 24 January 2019 (for the experiment of *PSII* photochemical efficiency). On the one hand, the sample of *S. arcuata* was collected at an irrigation canal at Shimochishiki-cho (0.1–0.3 m deep; 32°6'11.3"N 130°19'43.1"E) in Izumi City, Kagoshima Prefecture, Japan on 30 January and 28 February and 1 April 2017 (for the experiment of oxygenic photosynthesis) and 14 January 2019 (for the experiment of *PSII* photochemical efficiency). At the field survey, we also measured incident irradiance on the algae and river surface irradiance, respectively by using a spherical (4π) submersible quantum sensor (LI-192, LI-250A, LI-COR, Lincoln, Nebraska, USA). We note that the sample collection site at Katsume was the same as a previous study for *N. tortuosa* (Fujimoto *et al.* 2014).

Samples were collected in a manner to avoid influencing the abundance of the natural population; therefore, we minimized the number of specimens collected for each experiment. Approximately thirty individuals were collected at each sampling date and stored in 500 mL polycarbonate bottles with the freshwater from the study site. Bottles

were stored in a cooler at approximately the same temperature as the study site, and were transported to the laboratory. The samples were maintained for a few days before each experiment in 500 mL flasks at 16°C, which is approximately the same water temperature as that of sampling site on the sampling date. The flasks were filled with sterilized freshwater that was collected from the freshwater spring near the study site. The irradiance during the maintenance incubations was 50 μmol photons m^{-2} s^{-1} (12:12 h light: dark cycle; MTI-201B incubator, ELYA, Tokyo Rikakikai Co., Ltd., Tokyo, Japan).

2.2. Irradiance effect on the oxygenic photosynthesis

The methods for photosynthesis– irradiance (*P–E*) experiment followed a previous study (Terada *et al.* 2016). Photosynthetic rates of the samples in the present study were determined at nine levels of irradiance, 0, 5, 10, 30, 60, 100, 200, 500 and 1,000 μmol photons m^{-2} s^{-1} (provided by a metal-halide lamp, MHN-150D-S, Nichido Ind. Co. Ltd, Osaka, Japan), and with five replicates at 16°C (*T. okadae*, *V. helminthosa* and *S. arcuata*) and 20°C (*T. gaudichaudii*). Irradiance was measured with a spherical (4π) submersible quantum sensor. A water bath (Coolnit CL-600R, Taitec, Inc., Tokyo, Japan) was used to maintain experimental temperature.

To start the incubation, we placed five randomly selected individuals in

Biochemical Oxygen Demand (BOD) bottles (YSI-Japan's genuine model) containing 100 mL sterilized freshwater (note that the exact volume varies from each BOD bottle, which was accounted for in the analysis). The dissolved oxygen (DO) sensors were inserted into the bottles so that no bubbles were trapped. Water in the bottles was continuously stirred during the measurement. DO concentrations (mg L^{-1}) were measured every five minutes for 30 minutes, with 10 minutes of pre-incubation to each irradiance level, using DO meters equipped with optical DO sensors (ProODO-BOD, YSI Incorporated, Yellow Springs, Ohio, USA).

Dark respiration and net photosynthetic rates were determined by fitting a first-order linear model to the collected data, and were then normalized to the water volume of each BOD bottle and the fresh weight of each sample. The fresh weight of the samples used in this experiment were 508.2 ± 4.82, 421.3 ± 21.8, 48.8 ± 4.26, 502.3 ± 2.17 and 1393.1 ± 51.7 (mean ± SD) mg wet weight (mg_{ww}) for *T. okadae*, macroscopic and microscopic stage of *T. gaudichaudii*, *V. helminthosa* and *S. arcuata*, respectively. The freshwater medium was continuously stirred during the measurement, and was renewed for every change in irradiance to avoid any effects that could be attributed to the depletion of nutrients and dissolved carbon dioxide.

2.3. Temperature effect on the oxygenic photosynthesis

On the methods for photosynthesis–temperature (*P–T*) experiment, eight temperature treatments of 8, 12, 16, 20, 24, 28, 32 and 36°C with five replicates were examined under a saturating irradiance of 100 μmol photons m^{-2} s^{-1} (derived from *P–E* curve; Terada *et al.* 2016;). In addition, measurement at 40 and 44°C were also examined for macroscopic life-history stage of *T. gaudichaudii*. Temperature was manipulated with a temperature-controlled water bath (Coolnit CL-600R, Taitec, Inc., Tokyo, Japan) and DO was measured using an optical sensor equipped DO meter after 30-minute acclimation to each temperature condition. Rates in this experiment were likewise determined by fitting a first-order linear model to the collected data, and were then normalized to the water volume of each BOD bottle and the fresh weight of sample.

The fresh weight of the samples used in this experiment were 507.8 ± 8.02, 414.4 ± 12.1, 161.2 ± 10.3, 606.6 ± 9.42 and 1819.1 ± 68.7 (mean ± SD) mg wet weight (mg_{ww}) for *T. okadae*, two stages of *T. gaudichaudii*, *V. helminthosa* and *S. arcuata*, respectively. The freshwater medium was continuously stirred during the incubation, and was also renewed for every change in temperature to avoid any effects that can be attributed to the depletion of nutrients and dissolved carbon dioxide.

To determine the photosynthetic rates and dark respiration rates, the samples in

the bottles were first pre-incubated for 30 minutes to acclimate them to each experimental condition. The DO concentration (mg L^{-1}) was recorded every five minutes for 30 minutes. A linear model was fit to each of the concentrations with respect to time, and the slope estimated from the model provided an estimate of the photosynthetic rate. Hence, positive slopes occurred for photosynthesis and negative slopes were observed for dark respiration. All rates were then normalized to water volume of each BOD bottle and the fresh-weight of the sample.

2.4. Temperature response on the maximum quantum yield (F_v/F_m) of the Photosystem II (*PSII*)

Maxi and Mini Imaging-PAM (Heinz Walz GmbH, Effeltrich, Germany) measurements were based on procedures detailed in previous studies (Terada *et al*. 2016c, 2018, 2019). To elucidate how temperature affects *T. okadae* and *T. gaaudichaudii*, approximately 5-cm long portions of thalli (main axis) were placed in a stainless-steel tray (12cm × 10cm × 3 cm) with sterilized freshwater, providing for ten randomly selected measuring spots (ten replicates). Temperature was controlled with a block incubator (BI-535A, Astec, Fukuoka, Japan) by placing the stainless-steel tray on the aluminum block of the incubator. Water temperature in the stainless-steel tray was also measured with a thermocouple

(Model 925, testo AG, Lenzkirch, Germany) to confirm that the water reached the target temperature of the experiment. The maximum quantum yield (maximum photochemical efficiency of *PSII*, F_v/F_m; Cosgrove and Borowitzka 2011; ten replicates at each temperature level) was determined for temperatures of 8°C to 36 °C in 2 °C increments. The samples were allowed to acclimate for at least 30 minutes before measurements, after changes in water temperature and with at least ten minutes of the dark acclimation.

On the one hand, to elucidate how temperature affects *V. helminthosa* and *S. arcuata*, samples were acclimated overnight in the dark at 16°C. Thalli (n = 10 per temperature) were haphazardly selected and placed in a stainless-steel tray (12×10×3 cm) containing sterilized natural water. Water temperature in the tray was controlled with an aluminum block incubator (BI-536T, Astec, Fukuoka, Japan), and monitored with a thermocouple (testo 925, testo AG, Lenzkirch, Germany). After a 10-minute dark acclimation phase, F_v/F_m at 0 μmol photons m^{-2} s^{-1} were measured as initial values (initial F_v/F_m). Thalli were then placed in 500-mL flasks wrapped with aluminum foil and were incubated in the dark at eight temperatures (8, 12, 16, 20, 24, 28, 32, and 36°C) for 72 hours (EYELA MTI-201B, Tokyo Rikakikai Co., LTD., Tokyo, Japan). F_v/F_m at each temperature was measured at 24, 48, and 72 hours.

2.5. Combined effects of irradiance and temperature on quantum yields

The combined effects of irradiance and temperature on quantum yields for the samples were studied at some levels of irradiance (50, 100 and 1,000 μmol photons m^{-2} s^{-1}), and at some temperature treatments (12, 16, 22 and 24°C). The levels of temperature and irradiance were chosen based on the water temperature and light environment in the natural habitat of the study site (12 and 24°C under 100 and 1,000 μmol photons m^{-2} s^{-1} for *T. okadae*; 12 and 22°C under 50 and 1,000 μmol photons m^{-2} $s^{-1}$for *T. gaudichaudii*; 12, 16 and 24°C under 100 and 1,000 μmol photons m^{-2} $s^{-1}$for *V. helminthosa* and *S. arcuata*).

The samples were prepared following the same equipment described in the temperature–F_v/F_m experiment, with an initial overnight (12 hours) acclimation at each temperature condition in the dark, and subsequent measurement of initial F_v/F_m (n = 10 per treatment). Samples were placed in separate beakers (300 mL) containing sterile natural freshwater maintained at the specified temperatures in a water bath, and were exposed to 50, 100 or 1,000 μmol photons m^{-2} s^{-1} for 12 hours. The effective quantum yield in the *PSII* (Φ_{PSII}; n = 10 per treatment) were measured every two hours (including a measurement one-hour after the start of the experiment) of continuous exposure to each irradiance treatment. Following the experiment, samples were acclimated under the dark

(*T. okadae*, *T. gaudichaudi*) or dim light (*V. helminthosa* and *S. arcuata*; 20 μmol photons m^{-2} s^{-1}; Hanelt *et al*. 1997a,b; Schubert *et al.* 2015) for 12 hours at their respective temperatures; and their F_v/F_m were measured to confirm the possibility of recovery. Unfortunately, the value of Φ_{PSII} for *S. arcuata* in 6-h exposure under 100 μmol photons m^{-2} s^{-1} at 12°C were excluded from the results due the failure of measurement including the inappropriate setting of the equipment.

A one-way ANOVA was used to examine if continuous irradiance exposures affected Φ_{PSII} for each irradiance treatment and temperature condition. Time was considered a factor with levels: 0, 12, and 24 hours after the start of the experiment (*i.e.*, initial F_v/F_m, Φ_{PSII} after 12 h, and the final F_v/F_m after 12 hours of dark or dim light environment).

2.6. Modeling the photosynthetic response to irradiance and temperature

A Bayesian approach was used to analyze the response of photosynthesis to temperature. To model the response of either gross photosynthesis or maximum quantum yield to temperature, we applied a thermodynamic non-linear model (Equation 1), which assumes that photosynthesis enters a less active state above some optimal temperature (Thornley and Johnson 2000; Alexandrov and Yamagata 2007).

$$y = \frac{y_{max} \cdot H_d \cdot exp\left(\frac{H_a \cdot \left(K - K_{opt}\right)}{K \cdot R \cdot K_{opt}}\right)}{\left(H_d - H_a \cdot \left(1 - exp\left(H_d \cdot \frac{\left(K - K_{opt}\right)}{\left(K \cdot R \cdot K_{opt}\right)}\right)\right)\right)} \quad (1)$$

In this equation, y is the response variable, which is either the gross photosynthetic rate or the maximum quantum yield (F_v/F_m). The temperature scale is Kelvin (K). The model has four parameters: y_{max} scales the model to the range of y. K_{opt} is the absolute temperature where y is maximized, H_a is the activation energy in kJ mol^{-1} and H_d is the deactivation energy in kJ mol^{-1}. R in this model is the ideal gas constant and has a value of 8.314 J mol^{-1}. Although F_v/F_m is mathematically bounded by 0 and 1, we assumed y to be normally distributed, since the values were far from these limits. Gross photosynthetic rate, which is assumed as a hidden state, was estimated by simultaneously fitting the measured respiration rates to the Arrhenius equation (Equation 2), and the observed net photosynthetic rates to the difference between Equation 1 and 2. In the light, both photorespiration and non-photorespiratory (i.e., mitochondrial) reactions result in oxygen consumption (Tcherkez *et al*. 2008); however, it is not uncommon for the differences between respiration rates under light and dark conditions to be insignificant (Bellasio *et al*. 2014). Hence, photorespiration was assumed to be adequately described by the dark respiration rate. R_{24} is the respiration rate at 24°C and E_a is the activation energy. The constant 297.15 is 24°C scaled in absolute temperature.

$$R_d = R_{24} exp\left(-\frac{E_a}{R}\left(\frac{1}{K - 297.15}\right)\right) \quad (2)$$

The response of photosynthesis to irradiance was examined by modeling the data using an exponential equation (Jassby and Platt 1976; Webb *et al*. 1974; Platt *et al*. 1980; Henley 1993) that included a respiration term, and a term to model the effects of photoinhibition:

$$P_{net} = P_{max}\left(1 - exp\left(\frac{-\alpha}{P_{max}}E\right)\right)exp\left(\frac{-\beta}{P_{max}}E\right) - R_d \quad (3)$$

where, P_{net} was net O_2 production rate, P_{max} was maximum O_2 production rate, α was initial slope of the *P–E* curve, β was a parameter to model the effects of photoinhibition (set to 0 under conditions of no photoinhibition), E was incident irradiance, and R_d was the dark respiration rate. From this model, the saturation irradiance (E_k) was calculated as P_{max} / α, and the compensation irradiance (E_c) was $P_{max} ln\left(\frac{P_{max}}{(P_{max} - R_d)}\right)/\alpha$, when β is 0.

Statistical analyses of all the models were conducted using *R* v3.3.3 (R Development Core Team 2018), and model fitting was done using RStan v2.14.2 (Stan Development Team 2018). The parameters were determined by fitting the relevant models (*i.e.*, Equations 1-3) using Bayesian inference. RStan uses primarily a variant of a Hamiltonian Monte Carlo sampler to construct the posterior distributions of the

parameters, and four chains of at least 500,000 samples per chain were generated and assessed for convergence, which provided at least 1,000 samples of each of the parameters of interest. Informative normal priors were placed on all parameters of the model by using values from a previous study (Kokubu *et al.* 2015), and a half-Cauchy prior distribution was placed on the scale parameter of the models (Gelman 2004, 2006).

3. Results

3.1. *T. okadae*

3.1.1. Effect of irradiance on the oxygenic photosynthesis

The net photosynthetic rate at 16°C was modeled with Eq. 3, where a characteristic rise in NP rate occurred as irradiance increased (Fig. 3-1-1; Table 3-1-1). The modeled R_d was 1.35 μg O_2 g_{ww}^{-1} min^{-1} with a 95% Bayesian prediction interval (95% BPI) of 0.97–1.71 μg O_2

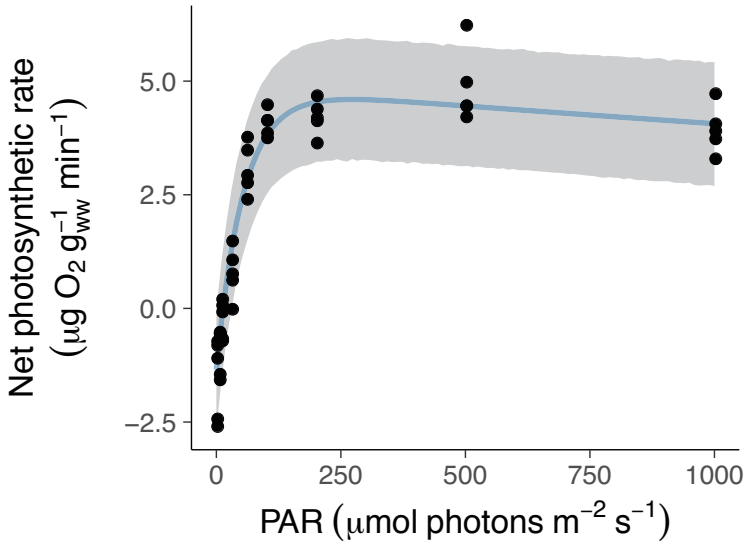

Fig. 3-1-1. Net photosynthetic rates of *Thorea okadae* with increasing irradiance (0–1,000 μmol photons m^{-2} s^{-1}) at 16°C. Dots indicate the measured rates (n = 5), line indicates expected value, and shaded region indicates the 95% Bayesian prediction interval (BPI).

g_{ww}^{-1} min^{-1}. Photosynthetic rates rapidly increased with increasing irradiance, where the initial slope (α) was 0.11 (0.09–0.14, 95% BPI) μg O_2 g_{ww}^{-1} min^{-1} (μmol photons m^{-2} s^{-1})$^{-1}$ and the compensation irradiance (E_c) was estimated to be 13.3 (10.3–16.3, 95% BPI) μmol photons m^{-2} s^{-1}. Photosynthetic rates saturated beyond 55.2 (42.2–72.9, 95% BPI) μmol photons m^{-2} s^{-1} (i.e., saturation irradiance E_k). The maximum net photosynthetic rate was estimated to be 4.60 (4.21 – 5.02, 95% BPI) μg O_2 g_{ww}^{-1} min^{-1}. A characteristic depression of the net photosynthetic rate was also observed at irradiance above the irradiance where the maximum net photosynthetic rate occurred.

Table 3-1-1. Mean and 95% Bayesian prediction intervals (95% BPI) of parameters estimated from the net photosynthesis–irradiance (*P–E*), gross photosynthesis–temperature (*P–T*), and the F_v/F_m–temperature model of *Thorea okadae*.

Parameters	Mean	95% BPI
NP_{max}	4.60	4.21 – 5.02
α	0.11	0.09 – 0.14
R_d	1.35	0.97 – 1.71
E_c	13.3	10.3 – 16.3
E_k	55.2	42.2 – 72.9
GP_{max}	17.3	16.1 – 18.6
H_a	43.5	37.4 – 50.4
H_d	627	485 – 800
$\boldsymbol{T_{opt}^{GP}}$	30.8	30.0 – 31.7
R_{22}	3.84	3.61 – 4.08
F_v/F_m	0.47	0.46– 0.48
H_a	8.21	5.97 – 11.2
H_d	177	154 – 201
$\boldsymbol{T_{opt}^{Fv/Fm}}$	18.4	17.0 – 19.8

3.1.2. Effect of temperature on the oxygenic photosynthesis and dark respiration

A clear single-peak temperature-dependent relationship between the net photosynthetic rates and temperature was observed, as well as an increase in dark respiration rates with increasing temperature (Fig. 3-1-2). Measured NP rates at 200 µmol photons m^{-2} s^{-1} increased from 3.40 ± 0.36 g O_2 g_{ww}^{-1} min^{-1} (mean ± SD) at 8°C to 9.57 ± 1.94 g O_2 g_{ww}^{-1} min^{-1} at 32°C, then decreased to –5.35 ± 3.32 g O_2 g_{ww}^{-1} min^{-1} at 36°C (Fig. 3-1-2). The dark respiration rate was –1.13 ± 0.23 g O_2 g_{ww}^{-1} min^{-1} at 8°C and increased to -10.5 ± 1.16 g O_2 g_{ww}^{-1} min^{-1} at 36°C (Fig. 3-1-2). The estimated gross photosynthetic rates fitted to the model increased with increasing temperatures and attained a maximum (GP_{max}) (17.3 (16.1 – 18.6, 95% BPI) µg O_2 g_{ww}^{-1} min^{-1}) at optimum temperature (T_{opt}^{GP}) of 30.8°C (30.0 – 31.7°C, 95% BPI), then sharply decreased (Fig. 3-1-2).

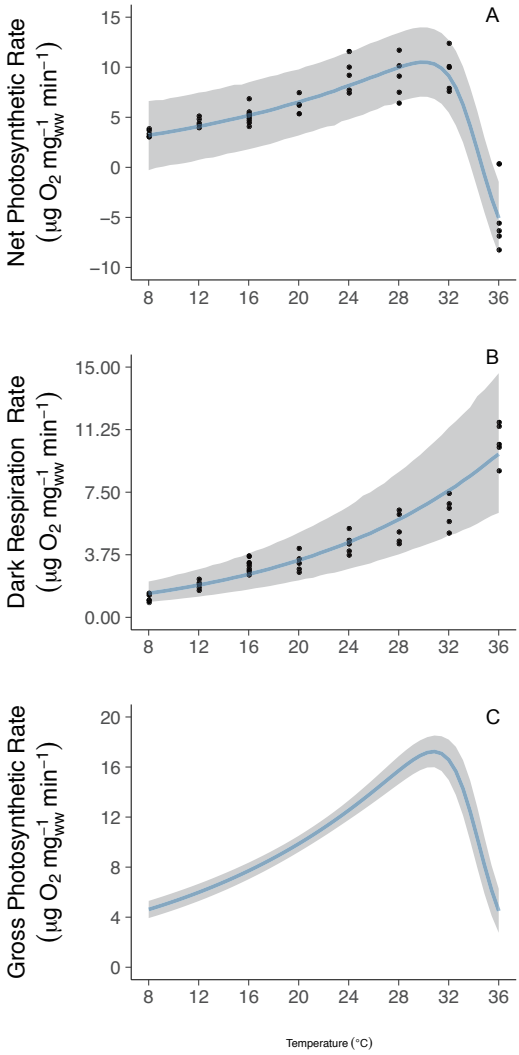

Fig. 3-1-2. Oxygenic photosynthesis and dark respiration of *Thorea okadae* at temperatures of 8–36 °C. Dots indicate measured rates (n = 5), lines indicate expected value, and shaded regions indicate 95% Bayesian prediction interval. **A:** Net photosynthetic rate determined at 200 µmol photons m^{-2} s^{-1}. **B:** Dark respiration rate at 0 µmol photons m^{-2} s^{-1}. **C:** Modeled gross photosynthetic rate determined at 200 µmol photons m^{-2} s^{-1}. Data were derived from model curve of net photosynthesis (**B**) and dark respiration (**C**).

The activation and deactivation energy parameters were 43.5 (37.4 – 50.4, 95% BPI) kJ mol^{-1} and 627 (485 – 800, 95% BPI) kJ mol^{-1}, respectively (Table 3-1-1).

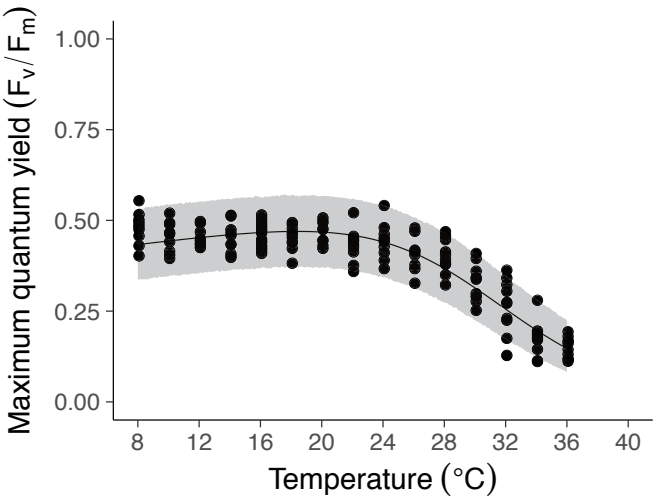

Fig. 3-1-3. Temperature response (8–36°C) of the maximum quantum yield (F_v/F_m) in the photosystem II in *Thorea okadae*. Dots indicate measured values (n = 10), line indicates expected value, and shaded region indicates the 95% BPI.

3.1.3. Temperature effect on the maximum quantum yield of PSII

The maximum quantum yield (F_v/F_m) was somewhat stable at low temperatures between 8 and 24 °C (Fig. 3-1-3), and decreased thereafter to a minimum of 0.15 ± 0.03 at 36 °C. However, a slight increase with increasing temperature and a subsequent slight decrease was detected. The model estimated that the maximum F_v/F_m of 0.47 (0.46 – 0.48, 95% BPI) had occurred at 18.4°C ($T_{opt}^{Fv/Fm}$; BPI: 17.0 – 19.7°C) for the gametophyte. The activation and deactivation energy were estimated to be 8.21 (5.97 – 11.2, 95%BPI) kJ mol^{-1} and 177 (154 – 201, 95%BPI) kJ mol^{-1} (Table 3-1-1).

3.1.4. Combined effects of irradiance and temperature on the effective and maximum quantum yield, and their potential of recovery

Responses of the Φ_{PSII} over 12 hours of continuous exposures to 100 and 1,000 μmol photons m^{-2} s^{-1} at 12°C and 24°C, and recovery of their F_v/F_m after a 12-hour dark acclimation phase were different from each irradiance-temperature treatment (Fig. 3-1-4).

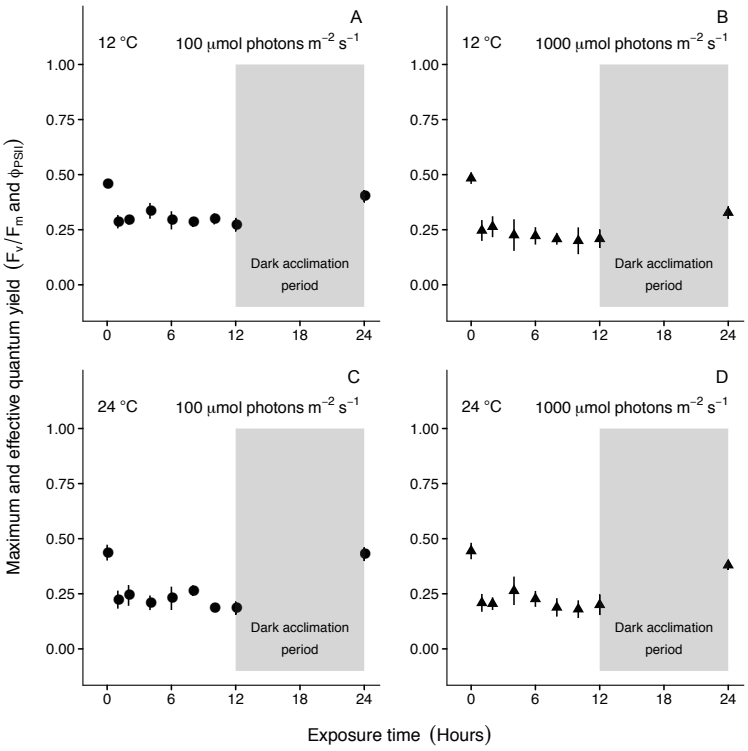

Fig. 3-1-4. Hourly response of effective quantum yield (Φ_{PSII}) in photosystem II in *Thorea okadae* to irradiance at 100 and 1,000 μmol photons m^{-2} s^{-1} at 12°C and 24°C. Symbols indicate average of actual values measured (n = 10), and bars indicate s. Initial values and values after overnight dark acclimation (12 h) were measured as maximum quantum yields (F_v/F_m). **A:** F_v/F_m and Φ_{PSII} measured before (initial state, F_v/F_m) and during 12 h irradiance exposure at 100 μmol photons m^{-2} s^{-1} (Φ_{PSII}), and after 12 h of dark acclimation (overnight recovery, F_v/F_m) at 12°C. **B:** 12 h irradiance exposure at 1,000 μmol photons m^{-2} s^{-1} (Φ_{PSII}), and after 12 h of dark acclimation at 12°C. **C:** 12 h irradiance exposure at 100 μmol photons m^{-2} s^{-1} (Φ_{PSII}), and after 12 h of dark acclimation at 24°C. **D:** 12 h irradiance exposure at 1,000 μmol photons m^{-2} s^{-1} (Φ_{PSII}), and after 12 h of dark acclimation at 24°C.

At 12°C, quantum yields after 12 hours of exposure to 100 μmol photons m^{-2} s^{-1} significantly declined ($P < 0.001$) from initial F_v/F_m of 0.46 ± 0.01 (mean ± SD) to Φ_{PSII} of 0.27 ± 0.03 (58.7%; Fig. 3-1-4). Those exposed to 1,000 μmol photons m^{-2} s^{-1} more declined more ($P < 0.001$) from 0.48 ± 0.03 (mean ± SD) to 0.21 ± 0.04 (43.8%; Fig. 3-1-4). Despite the rise in F_v/F_m to 0.40 ± 0.03 (at 100 μmol photons m^{-2} s^{-1}) and 0.33 ± 0.03 (at 1,000 μmol photons m^{-2} s^{-1}) following 12-hour

dark acclimation, values were still significantly different ($P < 0.001$) from the initial values. Post-dark acclimation F_v/F_m increased by 88.0 % for the low irradiance-treated samples, and by 67.7% for those under high irradiance.

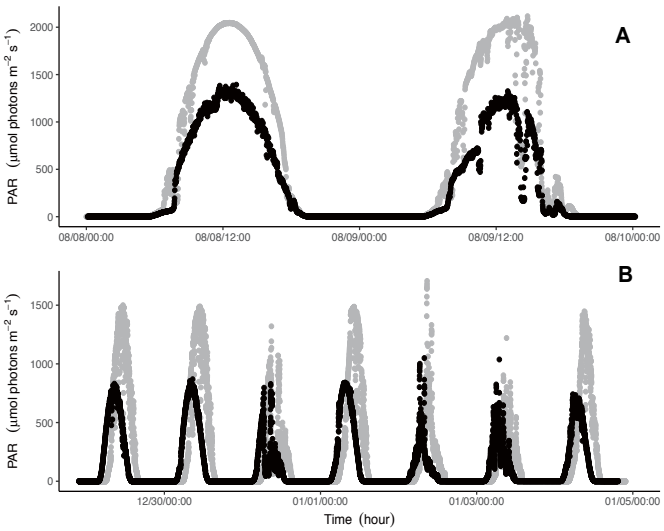

Fig. 3-1-5. Diurnal change of underwater riverbed irradiance (black dots) in the *Thorea okadae* population and river surface irradiance (grey dots), Hishikari, Sendai-gawa river, Kagoshima, Japan. Measurements were recorded every 1 second, and the average irradiance every minute was calculated. **A:** Diurnal change of irradiance E between 8 and 9 August 2015. **B:** Diurnal change of irradiance between 29 December 2015 and 4 January 2016.

At 24°C, quantum yields after 12 hours of exposure to 100 μmol photons m^{-2} s^{-1} significantly declined ($P < 0.001$) from an initial F_v/F_m of 0.44 ± 0.04 (mean ± SD) to Φ_{PSII} of 0.18 ± 0.03 (40.9%; Fig. 8). Those exposed to 1,000 μmol photons m^{-2} s^{-1} also significantly declined ($P < 0.001$) from 0.44 ± 0.04 (mean ± SD) to 0.20 ± 0.05 (45.5%; Fig. 3-1-4). After overnight dark acclimation, F_v/F_m of samples under low irradiance returned to its initial value (0.43 ± 0.03 SD). However, at high irradiance, F_v/F_m were still significantly different ($P < 0.001$) from the initial (0.38 ± 0.02 SD). Nevertheless, 98.3 % of the recovery from the initial was observed in the former treatment after 12-hour dark acclimation; meanwhile, those in the latter treatment was 85.5%.

3.1.5. Diurnal change of the *in situ* irradiance and water temperature in the study site

The diurnal change of *in situ* irradiance at the riparian zone, were measured on –9 August 2015 (summer) and 29 December to 4 January 2016 (winter) (Table 3-1-2, Fig. 3-1-5). On 8–9 August, sunrise was at 05:38, and sunset was 19:09 and 19:08, respectively. Weather was sunny with clear skies, except at early evening of 9 August. During measurement, the maximum and average *in situ* irradiance of the day were between 12:00 – 12:59 and were 1,392 and 1,311 μmol photons m^{-2} s^{-1}, respectively (Table 3-1-2). Meanwhile, the maximum terrestrial surface irradiance of the day and the average surface irradiance at 12:00 – 12:59 were 2,083 and 2,041 μmol photons m^{-2} s^{-1}, respectively. The daily integrated *in situ* and ground irradiance were 34,616 and 57,150 mmol photons m^{-2} d^{-1}, respectively.

As for *in situ* measurements during 29 December 2015 to 4 January 2016, sunrise was at 07:16 on 29 December and at 07:18 on 4 January. Sunset was at 17:23 and 17:28, respectively. Weather was sunny without clouds on 29–30 December, 1 and 4 January; weather was poor on other days. During measurement, maximum *in situ* irradiance of the day and the average *in situ* irradiance at 12:00 – 12:59 were 1,048 and 707 μmol photons

m^{-2} s^{-1}, respectively. Meanwhile, maximum ground irradiance of the day and the average ground irradiance at 12:00 – 12:59 were 1,706 and 1,173 μmol photons m^{-2} s^{-1}, respectively. The daily integrated rate of *in situ* and ground irradiance were 16,019 and 27,366 mmol photons m^{-2} d^{-1}, respectively.

Daily temperature measured at the study site ranged between 24.4°C and 28.3°C on 8 August, and between 24.3°C and 28.4°C on 9 August (Fig. 3-1-6). Temperatures during winter also showed diurnal fluctuations that ranged between 10.8°C and 13.1°C (Fig. 3-1-6). The highest and lowest temperatures during winter were 10.8°C and 15.7°C, respectively.

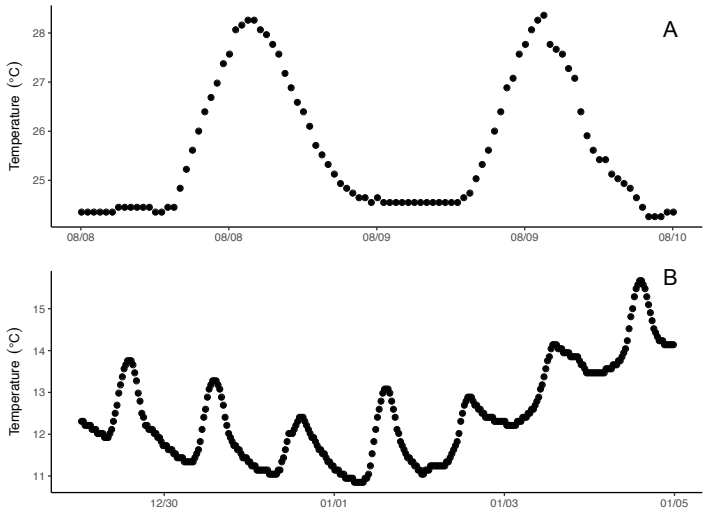

Fig. 3-1-6. Diurnal change of water temperature in *Thorea okadae* population, Hishikari, Sendai-gawa river, Kagoshima, Japan; measurements recorded every 30 min. **A:** Water temperature between 8 and 9 August 2015. **B:** Water temperature between 29 December 2015 and 4 January 2016.

Table 3-1-2. *In situ* irradiance on *Thorea okadae* population and the ground irradiance at the study site measured on 8–9 August 2015, and 29 December 2015 – 4 January 2016 at Sendai-gawa river, Kagoshima, Japan.

	Thorea okadae population					Ground Level					
	Integral of the *in situ* irradiance[a]	Maximum *in situ* irradiance[b] of the day		Average *in situ* irradiance[b] at 12:00 - 12:59		Integral of the ground irradiance[a]	Maximum ground irradiance[b] of the day		Average ground irradiance[b] at 12:00 - 12:59		
Date			Time		SD			Time		SD	
Aug. 8	34,616	1,392	13:02	1,311	31	57,150	2,045	12:33	2,041	3	Sunny
Aug. 9	24,711	1,322	12:49	1,205	182	47,717	2,083	14:41	2,007	49	P. Cloudy
Dec. 29	15,690	831	11:04	669	40	26,899	1,500	11:27	1,145	147	Sunny
Dec. 30	16,019	868	11:28	689	50	27,366	1,480	11:32	1,172	163	Sunny
Dec. 31	7,796	828	11:47	348	244	12,342	1,320	9:40	462	293	P. Cloudy
Jan. 1	15,737	838	10:44	707	49	24,586	1,480	11:19	1,173	250	Sunny
Jan. 2	6,447	1,048	11:38	153	25	10,953	1,706	10:13	276	43	Showers
Jan. 3	7,512	1,036	10:59	312	134	9,379	1,220	10:59	421	164	Showers
Jan. 4	12,242	740	9:51	552	65	21,574	1,447	11:14	1,126	121	P. Cloudy

[a] In mmol photons m^{-2} d^{-1}

[b] In μmol photons m^{-2} s^{-1}

3.2. *Thorea gaudichaudii*

3.2.1. Irradiance effect on the oxygenic photosynthesis

Measured net photosynthetic (NP) rates of two life-history stages at 20°C steadily increased and saturated as irradiance increased; from –1.88 ± 1.35 μg O_2 g_{ww}^{-1} min^{-1} (mean ± SD) at 0 μmol photons m^{-2} s^{-1} to 3.33 ± 0.38 μg O_2 g_{ww}^{-1} min^{-1} at 1,000 μmol photons m^{-2} s^{-1} for the macroscopic life-history stage (Fig. 3-2-1A), and from –1.76 ± 1.91 to 0.48 ± 2.12 μg O_2 g_{ww}^{-1} min^{-1} for the microscopic stage (Fig. 3-2-1B).

The parameter estimates that describe the significant features of each *P–E* curve were shown in Table 1. The maximum net photosynthesis (NP_{max}) of the macroscopic and microscopic life-history stages were 3.97 (3.57 – 4.40, 95% Bayesian Prediction Interval; BPI) μg O_2 g_{ww}^{-1} min^{-1} and 3.38 (2.25 – 4.48, BPI) μg O_2 g_{ww}^{-1} min^{-1}, respectively. Compensation (E_c) and saturation irradiance (E_k) of the macroscopic life-history stage were 6.71 (4.30 – 9.13, BPI) μmol photons m^{-2} s^{-1} and 26.6 (19.0 – 37.4, BPI) μmol photons m^{-2} s^{-1}; whereas those of the microscopic stage were

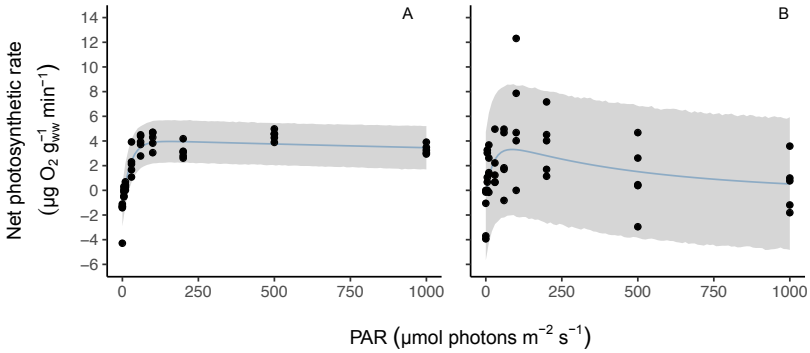

Fig. 3-2-1. The effect of irradiance (0–1,000 μmol photons m^{-2} s^{-1}) on oxygenic photosynthesis in macroscopic (**A**) and microscopic (**B**) life-history stages of *Thorea gaudichaudii* at 20°C. Dots indicate the measured rates (n = 5), line indicates expected value, and shaded region indicates the 95% Bayesian prediction interval (BPI).

2.56 (0.13 – 7.19, BPI) μmol photons m^{-2} s^{-1} and 30.0 (12.1 – 63.0, BPI) μmol photons m^{-2} s^{-1}, respectively. Other parameters were also shown in Table 3-2-1.

Table 3-2-1. Mean and 95% Bayesian prediction intervals (BPI) of parameters estimated from the net photosynthesis–irradiance (*P–E*) model of macroscopic and microscopic stages of *Thorea gaudichaudii*.

	Macroscopic stage		Microscopic stage	
Parameter	Mean	95% BPI	Mean	95% BPI
NP_{max}	3.97	3.57 – 4.40	3.38	2.25 – 4.48
α	0.20	0.14 – 0.28	0.18	0.08 – 0.32
R_d	1.20	0.69 – 1.69	0.41	0.36 – 1.06
E_c	6.71	4.30 – 9.13	2.56	0.13 – 7.19
E_k	26.6	19.0 – 37.4	30.0	12.1 – 63.0

NP_{max}: maximum net photosynthesis (μg O_2 g_{ww}^{-1} min^{-1}); α: initial slope of the *P–E* model (μg O_2 g_{ww}^{-1} min^{-1} [μmol photons m^{-2} s^{-1}]); R_d: respiration rate (μg O_2 g_{ww}^{-1} min^{-1}); E_c: compensation irradiance (μmol photons m^{-2} s^{-1}); E_k: saturation irradiance (μmol photons m^{-2} s^{-1}).

3.2.2. Temperature effect on the oxygenic photosynthesis

Photosynthesis–temperature (*P–T*) responses of two life-history stages showed a characteristic single peak, while dark respiration rates increased with rising temperature (Fig. 4-2). Measured NP rates of the macroscopic life-history stage at 100 μmol photons m^{-2} s^{-1} increased from 1.60 ± 0.53 μg O_2 g_{ww}^{-1} min^{-1} (mean ± SD) at 8°C to 2.24 ± 0.54 μg O_2 g_{ww}^{-1} min^{-1} at 32°C, then decreased to –3.29 ± 1.55 μg O_2 g_{ww}^{-1} min^{-1} at 44°C (Fig. 3-2-2A). Meanwhile, NP rates of the microscopic stage at 100 μmol photons m^{-2} s^{-1}

increased from 2.42 ± 0.25 µg O_2 g_{ww}^{-1} min^{-1} at 8°C to3.78 ± 1.08 µg O_2 g_{ww}^{-1} min^{-1} at 28°C, then decreased to 2.04± 0.97 µg O_2 g_{ww}^{-1} min^{-1} at 36°C (Fig. 3-2-2B).

The dark respiration rate of the macroscopic stage was 0.23 ± 0.18 µg O_2 g_{ww}^{-1} min^{-1} at 8°C; it peaked to 2.38 ± 1.80 µg O_2 g_{ww}^{-1} min^{-1} at 44°C (Fig. 3-2-2C). As for the microscopic stage, it was –0.04 ± 0.74 µg O_2 g_{ww}^{-1} min^{-1} at 8°C and increased to 3.31 ± 0.81 µg O_2 g_{ww}^{-1} min^{-1} at 36°C (Fig. 3-2-2D).

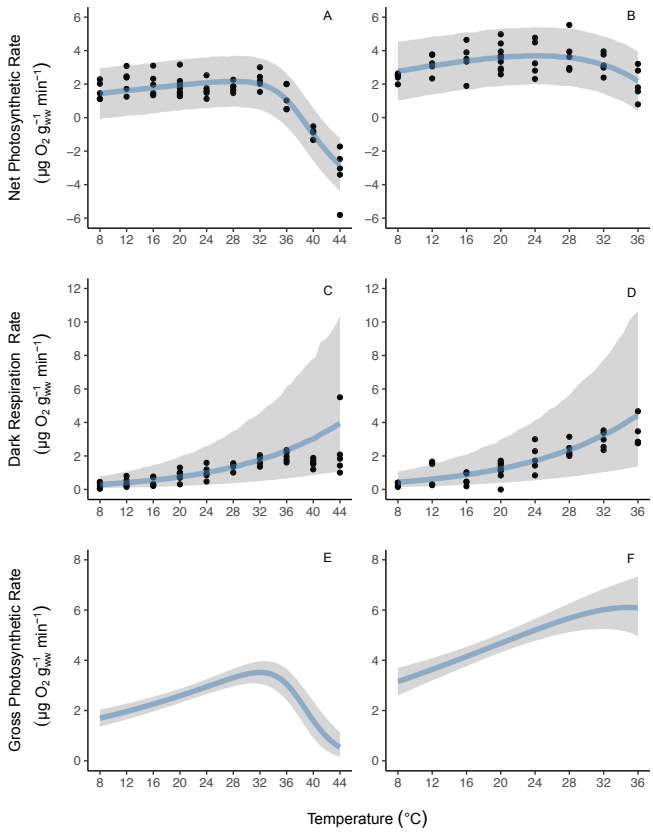

Fig. 3-2-2. The effect of temperature on oxygenic net photosynthesis (**A, B**), dark respiration (**C, D**) and gross photosynthesis (**E. F**) in macroscopic (**A, C, E**) and microscopic (**B, D, F**) life-history stages of *Thorea gaudichaudii*. The net and gross photosynthetic rates determined at 100 µmol photons m^{-2} s^{-1}. Dots indicate the measured rates (n = 5), line indicates expected value, and shaded region indicates the 95% BPI. Experiments were conducted at ten temperature treatments between 8 and 44°C for two life-history stages; however, those at 40 and 44°C for microscopic stage was excluded from the results due to the failure of temperature control.

Parameter estimates for the *P–T* model are shown in Table 3-2-2. Briefly, the maximum gross photosynthesis (GP_{max}) of the macroscopic life-history stage was 3.54 (3.10 – 3.99, BPI) µg O_2 g_{ww}^{-1} min^{-1} at the optimum temperature (T_{opt}^{GP}) of 32.1°C (29.8 – 34.0°C, BPI; Fig. 3-2-2E). Meanwhile, GP_{max} of the microscopic stage was 6.34 (5.31 –

8.21, BPI) μg O_2 g_{ww}^{-1} min^{-1} at 35.7°C (29.5 – 48.6°C, BPI; Fig. 3-2-2F).

Table 3-2-2. Mean and 95% BPI of parameters estimated from the gross photosynthesis–temperature (*P–T*) model of macroscopic and microscopic stages of *Thorea gaudichaudii*.

	Macroscopic stage		Microscopic stage	
Parameter	Mean	95% BPI	Mean	95% BPI
GP_{max}	3.54	3.10 – 3.99	6.34	5.31 – 8.21
H_a	24.2	17.2 – 32.7	26.6	14.9 – 56.6
H_d	332	220 – 464	133	51 – 292
T_{opt}^{GP}	32.1	29.8 – 34.0	35.7	29.5 – 48.6
R_{mean}	0.99	0.86 – 1.14	1.28	1.09 – 1.49

GP_{max}: maximum gross photosynthesis (μg O_2 g_{ww}^{-1} min^{-1}); H_a: activation energy for photosynthesis (kJ mol^{-1}); H_d: deactivation energy (kJ mol^{-1}); T_{opt}^{GP} : optimum temperature of oxygenic gross photosynthesis; R_{mean}: respiration rate at mean temperature.

3.2.3. Temperature response on the maximum quantum yield (F_v/F_m) of *PSII*

The responses of the maximum quantum yields of *PSII* (F_v/F_m) to temperature of macroscopic and microscopic life history stages are shown in Fig. 3-2-3. Measured F_v/F_m of the macroscopic life-history stage was highest at 14°C with 0.55 ± 0.01 SD and was likely stable above 0.51 during 8~26°C, and it decreased to a minimum of 0.31 ± 0.03 SD at 36°C. Meanwhile, F_v/F_m of the microscopic stage were less sensitive temperature, slightly decreased to a minimum of 0.50 ± 0.04 SD at 36°C.

Based on the model-fitted F_v/F_m – temperature curves, the maximum F_v/F_m of

0.54 (0.54 – 0.55, BPI) occurred at the optimum temperature of 17.8°C ($T_{opt}^{Fv/Fm}$; BPI: 16.7 – 18.8°C) for the macroscopic life-history stage. As for the microscopic stage, its maximum F_v/F_m of 0.62 (BPI: 0.61 – 0.63) was at 15.0°C (BPI: 12.3 – 17.1°C). Other model parameter estimates are presented in Table 3-2-3.

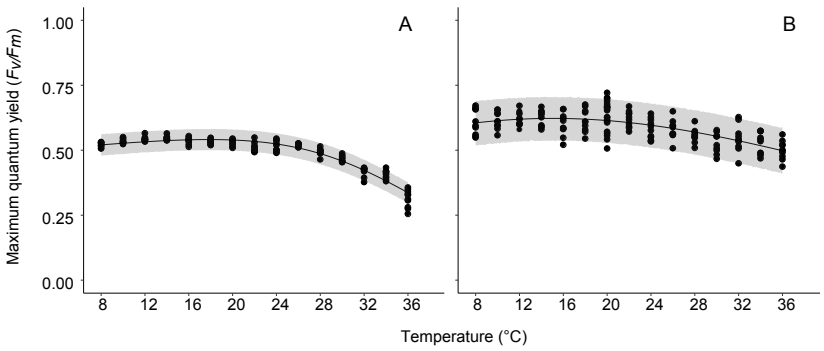

Fig. 3-2-3. The relationship between temperature (8–36°C) and the maximum quantum yield (F_v/F_m) in macroscopic (**A**) and microscopic (**B**) life-history stages of *Thorea gaudichaudii* under the thirty-minute temperature exposure. Dots indicate the measured values (n = 10 at each level), line indicates expected value, and shaded region indicates the 95% BPI.

Table 3-2-3. Mean and 95% BPI of parameters estimated from the F_v/F_m–temperature model of macroscopic and microscopic stages of *Thorea gaudichaudii*.

	Macroscopic stage		Microscopic stage	
Parameter	Mean	95 % BPI	Mean	95 % BPI
F_v/F_m	0.54	0.54 – 0.55	0.62	0.61 – 0.63
H_a	5.07	4.57 – 6.65	20.3	5.20 – 55.4
H_d	126	111 – 141	54.5	42.6 – 74.8
$T_{opt}^{Fv/Fm}$	17.8	16.7 – 18.8	15.0	12.3 – 17.1

F_v/F_m: maximum quantum yield; H_a: activation energy for photosynthesis (kJ mol^{-1}); H_d: deactivation energy (kJ mol^{-1}); $T_{opt}^{Fv/Fm}$: optimum temperature of the maximum quantum yield.

3.2.4. Combined effects of irradiance and temperature on quantum yields

Responses of the Φ_{PSII} over 12 hours of continuous exposure to 50 (low irradiance) and 1,000 µmol photons m^{-2} s^{-1} (high irradiance) at 12°C and 22°C, and their recovery of F_v/F_m after 12-hour dark acclimation are shown in Figs 3-2-4 and 3-2-5 (macroscopic and microscopic life-history stages, respectively).

For macroscopic stage, the initial values of F_v/F_m at each irradiance – temperature treatment were 0.42±0.03 SD (12°C, 50 µmol photons m^{-2} s^{-1}) – 0.51±0.02 SD (22°C, 1,000 µmol photons m^{-2} s^{-1}; Fig. 3-2-4). The Φ_{PSII} of two treatments under high irradiance significantly declined from initial F_v/F_m to Φ_{PSII} of 0.13 ± 0.02 SD at 12°C (P < 0.001; 33.0%) and of 0.15 ± 0.03 SD at 22°C (P < 0.001; 30.0%), and F_v/F_m did not recover to the initial state after 12-h of dark acclimation (P < 0.001; 28.5% at 12°C; 37.4% at 22°C; Fig. 3-2-4B, D), suggesting high irradiance stress. Meanwhile,

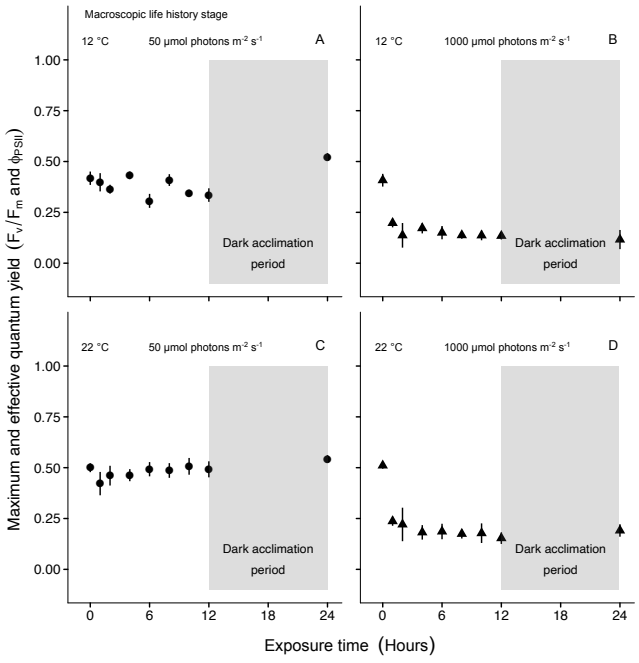

Fig 3-2-4. Hourly response of effective quantum yield (Φ_{PSII}) in macroscopic life-history stages of *Thorea gaudichaudii* to irradiance at 50 (**A, C**) and 1,000 µmol photons m^{-2} s^{-1} (**B, D**) at 12°C (**A, B**) and 22°C (**C, D**). Symbols indicate average of actual values measured (n = 10), and bars indicate standard deviation (SD). Initial values and values after overnight dark acclimation (12 h) were measured as F_v/F_m.

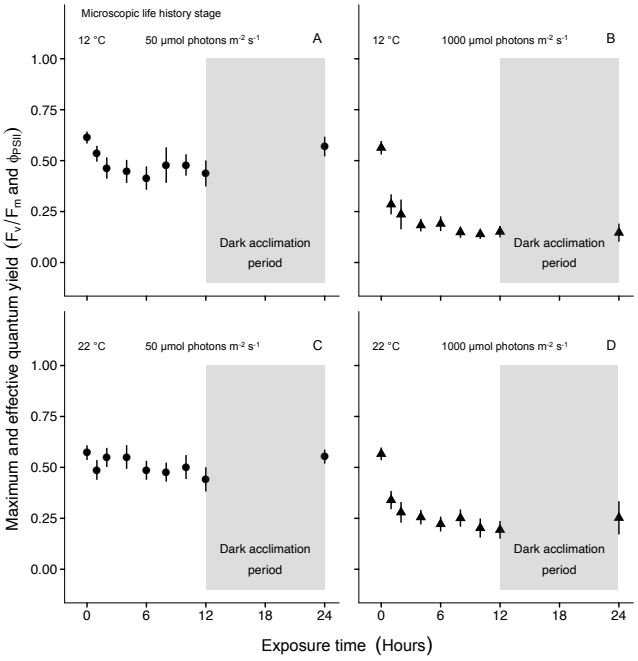

Fig 3-2-5. Hourly response of Φ_{PSII} in microscopic life-history stages of *Thorea gaudichaudii* to irradiance at 50 (**A, C**) and 1,000 µmol photons m^{-2} s^{-1} (**B, D**) at 12°C (**A, B**) and 22°C (**C, D**). Symbols indicate average of actual values measured (n = 10), and bars indicate SD. Initial values and values after overnight dark acclimation (12 h) were measured as F_v/F_m.

under low irradiance, the Φ_{PSII} remained to stabilize at close to the initial value over the 12-h exposure, Φ_{PSII} was 0.34 ± 0.03 SD at 12°C (P < 0.001; 80.2%) and 0.49 ± 0.04 SD at 22°C (P = 0.541; 98.4%); however, those under the chronic exposure at 12°C showed lower values than those at 22°C (Fig. 3-2-4A, C). F_v/F_m after 12-h of dark acclimation at 12°C and 22°C recovered over the initial state after 12-h of dark acclimation at 12°C (P < 0.001; 124.9%; Fig. 3-2-4A) and 22°C (P < 0.01; 108.7%; Fig. 3-2-4C).

For microscopic stage, the initial values of F_v/F_m at each irradiance – temperature treatment were 0.56±0.03 SD (12°C, 1,000 µmol photons m^{-2} s^{-1}) – 0.61±0.03 SD (12°C, 50 µmol photons m^{-2} s^{-1}; Fig. 3-24-5). Like the macroscopic stage, Φ_{PSII} of two treatments under high irradiance significantly declined from initial F_v/F_m to Φ_{PSII} of 0.15 ± 0.03 SD at 12°C (P < 0.001; 26.8%) and of 0.19 ± 0.04 SD at 22°C (P < 0.001; 34.2%), and F_v/F_m

did not recover to the initial state after 12-h of dark acclimation ($P < 0.001$; 26.0% at 12°C; 44.6% at 22°C; Fig. 3-2-5B, D). In contrast, under low irradiance, the Φ_{PSII} remained to stabilize at near the initial value over the 12-h exposure, Φ_{PSII} was 0.44 ± 0.06 SD at 12°C ($P < 0.001$; 71.2%) and 0.44 ± 0.06 SD at 22°C ($P < 0.001$; 77.1%), and F_v/F_m almost recovered to the initial state after 12-h of dark acclimation at 12°C ($P = 0.057$; 92.8%; Fig. 3-2-5A) and 22°C ($P= 0.348$; 96.6%; Fig. 4-5C).

3.2.5 *In situ* measurements of diurnal changes in photosynthetic activity

T. gaudichaudii was found in the concrete-reinforced basin fed by a freshwater spring. Freshwater was welling up continuously from the source of spring and the depth of water in the basin was around 30 cm. Inside the spring, these individuals were found attached to pebbles and also on the wall of basin; however, due to the shading by the basin wall, surrounding vegetation and the embankment that surrounded the study site, only a few minutes of direct sunlight could irradiate the algae. There were both macroscopic and microscopic stages in the habitat; however, due to the size of the microscopic stages, field measurement of chlorophyll fluorescence was done only for the macroscopic stage.

Underwater irradiance on the thallus showed diurnal changes during the field measurements (Fig. 3-2-6A). Levels increased from morning (irradiance at 10:28 – 10:30

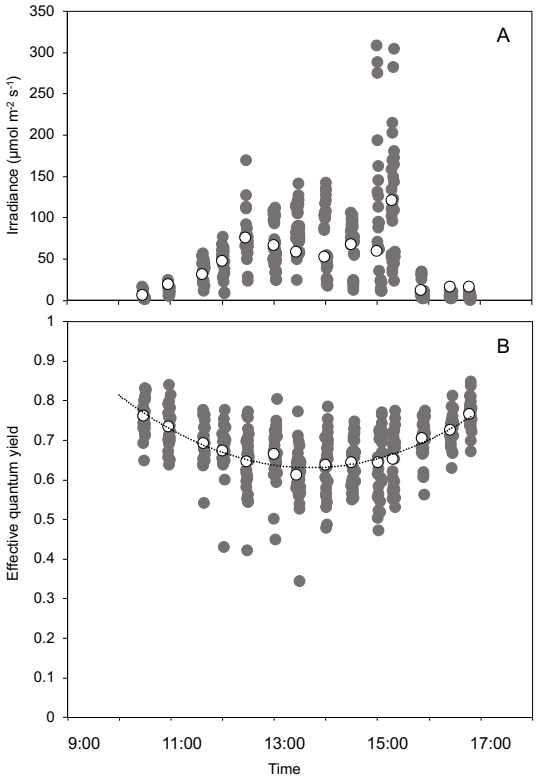

Fig. 4-6. Incident irradiance and Φ_{PSII} measurements conducted at a freshwater spring of "*Ufukubuga*", Okinawa-jima island on 11 May 2019 by using the Diving-PAM. **A**. Diurnal change of the incident irradiance on the frond of *Thorea gaudichaudii*. The grey and white symbols indicate actual values and hourly mean values of the measurement. **B**. Diurnal change of Φ_{PSII} of *T. gaudichaudii* taken *in situ.* The grey and white symbols indicate actual values and hourly mean values of the measurement, respectively, the line indicates the expected value determined by the locally estimated scatterplot smoothing (LOESS) smoothing.

= 5.35 ± 4.45 µmol photons m^{-2} s^{-1} SD) to the noon (irradiance at 12:27 – 12:30 = 75.7 ± 28.8 µmol photons m^{-2} s^{-1} SD), and then gradually decreased until the early evening (irradiance at 16:47 – 16:49 = 15.8 ± 10.6 µmol photons m^{-2} s^{-1} SD) except for the measurement near 15:00 where a some sunlight directly irradiate the surface of the water through a gap in the trees (irradiance at 15:17 – 15:21 = 120.3 ± 72.6 µmol photons m^{-2} s^{-1} SD).

In contrast, the Φ_{PSII} showed a diurnal decline and recovery during the day (Fig. 3-2-6B). Values at the start of measurement was relatively high (Φ_{PSII} = 0.767 ± 0.052 SD at 10:28 – 10:30), and then gradually decreased over time by noon and early afternoon (minimum Φ_{PSII} = 0.612 ± 0.068 SD at 13:26 – 13:30); thereafter, it recovered at the end of measurements (Φ_{PSII} = 0.765 ± 0.040 SD at 16:47 – 16:49). The diurnal change of hourly mean Φ_{PSII} was fitted to the following

equation: $y = 7.666x^2 – 8.7513x + 3.1285$ ($R^2 = 0.9414$). In so doing, Φ_{PSII} was negatively correlated with irradiance ($y = -0.0009x + 0.725$, $R^2 = 0.317$).

3.3. Two species of Batracospermaceae

3.3.1. Incident irradiance on the habitat

On 16 February 2017 (11:30 – 12:30), underwater incident irradiance on the thalli of *V. helminthosa* under shaded environment (along the vertical wall) was 61.2 ± 4.28 μmol photons m^{-2} s^{-1} (*n*=5; mean ± SD), and those on the canal floor under no shade was 1,501 ± 142.3 μmol photons m^{-2} s^{-1}. *V. helminthosa* was commonly found under the shaded habitat; nevertheless, it was also patchily found on the canal floor without shade. Incidentally, irradiance on the river surface was 2,283 ± 18.0 μmol photons m^{-2} s^{-1} during this time. Weather was fine without clouds.

On 28 February 2017 (13:00 – 13:30), underwater incident irradiance on the thalli of *S. arcuata* under shaded environment (along the vertical wall) was 174.4 ± 9.07 μmol photons m^{-2} s^{-1} (*n*=5; mean ± SD), and those on the canal floor under no shade was 1,639 ± 24.9 μmol photons m^{-2} s^{-1}. Like *V. helminthosa*, *S. arcuata* was also dominant at the shaded habitat; nevertheless, it was also patchily found on the canal floor without shade. Incidentally, irradiance on the water surface was 2,260 ± 37.8 μmol photons m^{-2} s^{-1} during this time. Weather was also fine without clouds.

3.3.2. Irradiance effect on the oxygenic photosynthesis

Measured net photosynthetic (NP) rates of *V. helminthosa* and *S. arcuata* at 16°C steadily increased and saturated as irradiance increased; from –0.68 ± 0.18 μg O_2 g_{ww}^{-1} min^{-1} (mean ± SD) at 0 μmol photons m^{-2} s^{-1} to 1.29 ± 0.13 μg O_2 g_{ww}^{-1} min^{-1} at 100 μmol photons m^{-2} s^{-1}, 1.30 ± 0.17 μg O_2 g_{ww}^{-1} min^{-1} at 1,000 μmol photons m^{-2} s^{-1} for *V. helminthosa* (Fig. 3-3-1A), and from –0.32 ± 0.07 at 0 μmol photons m^{-2} s^{-1} to 0.39 ± 0.10 μg O_2 g_{ww}^{-1} min^{-1} at 100 μmol photons m^{-2} s^{-1}, 0.29 ± 0.04 μg O_2 g_{ww}^{-1} min^{-1} at 1,000 μmol photons m^{-2} s^{-1} for *S. arcuata* (Fig. 3-3-1B).

The maximum net photosynthesis (NP_{max}) of *V. helminthosa* and *S. arcuata* were 1.30 (1.22 – 1.39, 95% Bayesian Prediction Interval; BPI) μg O_2 g_{ww}^{-1} min^{-1} and 0.38 (0.33 – 0.43, BPI) μg O_2 g_{ww}^{-1} min^{-1}, respectively (Table 3-3-1). Compensation (E_c) and saturation irradiance (E_k) of *V. helminthosa* were 6.95 (5.58 – 8.42, BPI) μmol photons m^{-2} s^{-1} and 18.8 (14.5 – 24.7, BPI) μmol photons m^{-2} s^{-1}; whereas those of *S. arcuata* were 11.5 (9.10 – 14.2, BPI) μmol photons m^{-2} s^{-1} and 17.7 (13.0 – 23.9, BPI) μmol photons m^{-2} s^{-1},

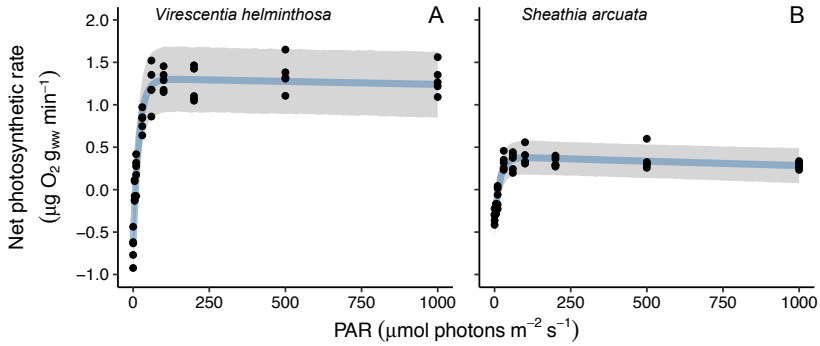

Fig. 3-3-1. The effect of photosynthetically active radiation (0–1,000 μmol photons m^{-2} s^{-1}) on oxygenic photosynthesis of *Virescentia helminthosa* (**A**) and *Sheathia arcuata* (**B**) at 16°C. Dots indicate the measured rates (n = 5), line indicates expected value, and shaded region indicates the 95% Bayesian prediction interval (BPI).

respectively.

Table 3-3-1. Mean and 95% Bayesian prediction intervals (95% BPI) of parameters estimated from the net photosynthesis–photosynthetically active radiation (*P–E*) model of *Virescentia helminthosa* and *Sheathia arcuata* from Kagoshima, Japan.

	Virescentia helminthosa		*Sheathia arcuata*	
Parameter	Mean	95 % BPI	Mean	95 % BPI
P_{max}	1.3	1.22 – 1.39	0.38	0.33 – 0.43
α	0.10	0.07 – 0.14	0.04	0.03 – 0.06
R_d	0.59	0.44 – 0.74	0.36	0.29 – 0.44
E_c	6.95	5.58 – 8.42	11.5	9.10 – 14.2
E_k	18.8	14.5 – 24.7	17.7	13.0 – 23.9

P_{max}: maximum net photosynthesis (μg O_2 g_{ww}^{-1} min^{-1}); α: initial slope of the *P–E* model (μg O_2 g_{ww}^{-1} min^{-1} [μmol photons m^{-2} s^{-1}]); R_d: respiration rate (μg O_2 g_{ww}^{-1} min^{-1}); E_c: compensation irradiance (μmol photons m^{-2} s^{-1}); E_k: saturation irradiance (μmol photons m^{-2} s^{-1}).

3.3.3. Temperature effect on the oxygenic photosynthesis

Photosynthesis–temperature (*P–T*) responses of *V. helminthosa* and *S. arcuata* showed a characteristic single peak, while dark respiration rates increased with rising temperature (Fig. 3-3-2). Measured NP rates of *V. helminthosa* at 100 μmol photons m^{-2} s^{-1} increased from 0.70 ± 0.31 μg O_2 g_{ww}^{-1} min^{-1} (mean ± SD) at 8°C to 1.13 ± 0.24 μg O_2 g_{ww}^{-1} min^{-1} at 20°C, then decreased to –0.15 ± 0.12 μg O_2 g_{ww}^{-1} min^{-1} at 36°C (Fig. 3-3-2A). Meanwhile, NP rates of *S. arcuata* at 100 μmol photons m^{-2} s^{-1} increased from 0.33 ± 0.09 μg O_2 g_{ww}^{-1} min^{-1} at 8°C to 0.69 ± 0.11 μg O_2 g_{ww}^{-1} min^{-1} at 28°C, then decreased to 0.18 ± 0.04 μg O_2 g_{ww}^{-1} min^{-1} at 36°C (Fig. 3-3-2B).

The dark respiration rate of *V. helminthosa* was 0.29 ± 0.15 µg O_2 g_{ww}^{-1} min^{-1} at 8°C; it peaked to 0.93 ± 0.29 µg O_2 g_{ww}^{-1} min^{-1} at 28°C (Fig. 3-3-2C). As for *S. arcuata*, it was 0.12 ± 0.04 µg O_2 g_{ww}^{-1} min^{-1} at 8°C and increased to 0.69 ± 0.31 µg O_2 g_{ww}^{-1} min^{-1} at 36°C (Fig. 3-3-2D).

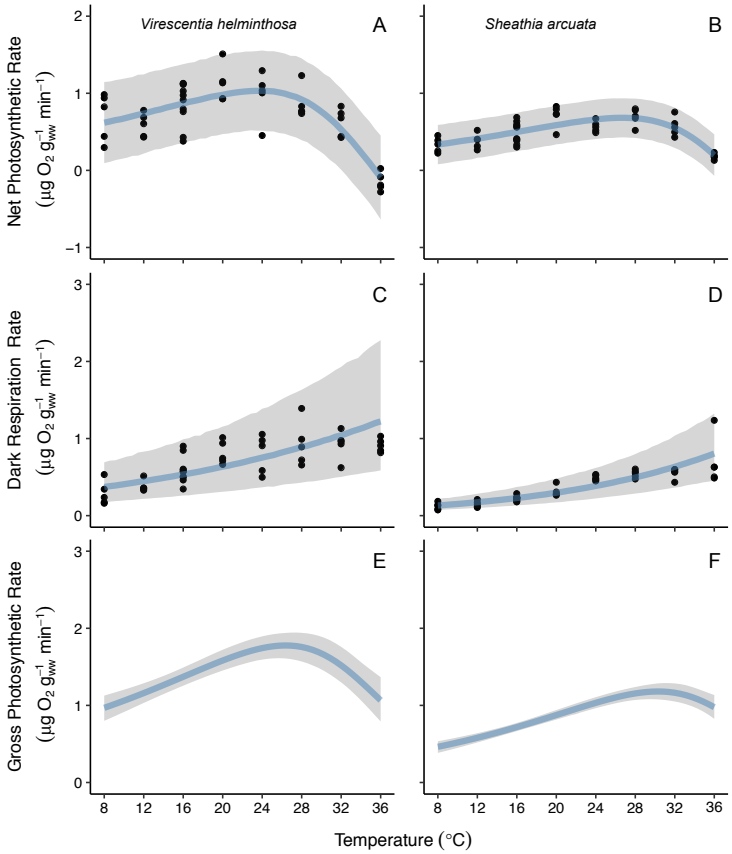

Fig. 3-3-2. The effect of temperature on oxygenic net photosynthesis (**A, B**), dark respiration (**C, D**) and gross photosynthesis (**E. F**) of *Virescentia helminthosa* (**A, C, E**) and *Sheathia arcuata* (**B, D, F**). The net and gross photosynthetic rates determined at 100 µmol photons m^{-2} s^{-1}. Dots indicate the measured rates (n = 5), line indicates expected value, and shaded region indicates the 95% Bayesian prediction interval (BPI).

The maximum gross photosynthesis (GP_{max}) of *V. helminthosa* that was estimated from the *P–T* model was 1.79 (1.62 – 1.96, BPI) µg O_2 g_{ww}^{-1} min^{-1} at the optimum temperature (T_{opt}^{GP}) of 26.4°C (23.9 – 28.7°C, BPI; Fig. 2E; Table 2). Meanwhile, GP_{max} of *S. arcuata* was 1.19 (1.08 – 1.29, BPI) µg O_2 g_{ww}^{-1} min^{-1} at 30.3°C (28.3 – 32.1°C, BPI; Fig. 3-3-2F; Table 3-3-2).

Table 3-3-2. Mean and 95% Bayesian prediction intervals (95% BPI) of parameters estimated from the gross photosynthesis–temperature (*P–T*) model of *Virescentia helminthosa* and *Sheathia arcuata* from Kagoshima, Japan.

	Virescentia helminthosa		*Sheathia arcuata*	
Parameter	Mean	95 % BPI	Mean	95 % BPI
GP_{max}	1.79	1.62 – 1.96	1.19	1.08 – 1.29
H_a	31.7	19.7 – 52.5	39.0	28.0 – 60.7
H_d	188	116 – 291	195	102 – 340
T_{opt}^{GP}	26.4	23.9 – 28.7	30.3	28.3 – 32.1
R_{mean}	0.65	0.59 – 0.72	0.33	0.30 – 0.35

GP_{max}: maximum gross photosynthesis (μg O_2 g_{ww}^{-1} min^{-1}); H_a: activation energy for photosynthesis (kJ mol^{-1}); H_d: deactivation energy (kJ mol^{-1}); T_{opt}^{GP}: optimum temperature of oxygenic gross photosynthesis; R_{mean}: respiration rate at mean temperature.

3.3.4. Temperature response on the maximum quantum yield (F_v/F_m) of *PSII*

Throughout the 72-hour different temperature exposures, F_v/F_m of *PSII* for two species remained steady at values around 0.5 from 8 to 24°C; however, it gradually decreased and dropped at more higher temperatures (Fig. 3-3-3).

For *V. helminthosa*, the values of F_v/F_m at 36°C were 0.20 ± 0.02 and 0.01 ± 0.01 SD at 24-h and 48-h exposures, respectively; thereafter, it dropped to zero at 72-h exposure. Likewise, those at 32°C were 0.31 ± 0.04 SD at 24-h exposure; however, it also dropped to 0.04 ± 0.02 SD and zero at 48-h and 72-h exposures, respectively. Given the model and data after 72 hours, maximum F_v/F_m of *V. helminthosa* was estimated to be 0.52 (0.49 – 0.54, BPI), and occurred at 18.5°C (17.1 – 19.7, BPI; $T_{opt}^{Fv/Fm}$; Table 3-3-3). Other model parameter estimates at 72 hours and those at 24 and 48 hours are presented

in Table 3-3-3~5.

For *S. arcuata*, values of F_v/F_m at 36°C were 0.05 ± 0.02 and 0.02 ± 0.00, and 0.02 ± 0.01 SD at 24-h, 48-h and 72-h exposures. Likewise, those at 32°C were 0.36 ± 0.03 and 0.24 ± 0.08 SD at 24-h and 48-h exposures; thereafter, it also dropped to 0.09 ± 0.07 SD at 72-h exposure. Given the model and data after 72 hours, maximum F_v/F_m of *S. arcuata* was estimated to be 0.56 (0.54 – 0.58, BPI), and occurred at 20.9°C (19.8 – 21.9, BPI; $T_{opt}^{Fv/Fm}$; Table 3-3-3). Other model parameter estimates at 72 hours and those at 24 and 48 hours are presented in Table 3-3-3~5.

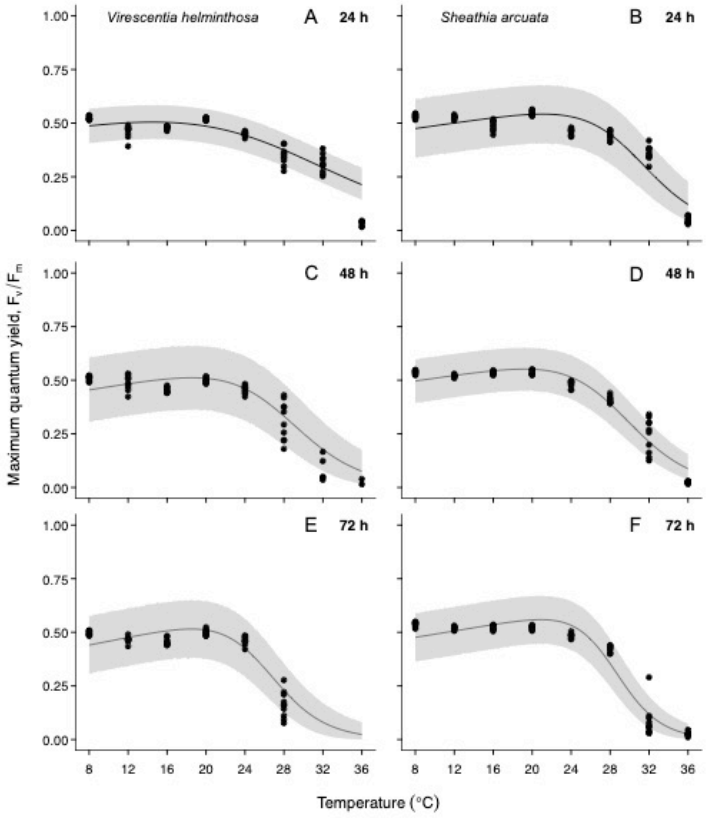

Fig. 3-3-3. The relationship between temperature (8–36°C) and the maximum quantum yield (F_v/F_m) of the Photosystem II (*PSII*) in *Virescentia helminthosa* (**A, C, E**) and *Sheathia arcuata* (**B, D, F**) under the 24-h (**A, B**), 48-h (**C, D**) and 72-h (**E, F**) temperature exposures. Dots indicate the measured values (n = 10 at each level), line indicates expected value, and shaded region indicates the 95% Bayesian prediction interval (BPI).

Table 3-3-3. Mean and 95% Bayesian prediction intervals (95% BPI) of parameters estimated from the F_v/F_m–temperature model of *Virescentia helminthosa* and *Sheathia arcuata* from Kagoshima,

Japan after 24-h exposure.

	Virescentia helminthosa		*Sheathia arcuata*	
Parameter	Mean	95 % BPI	Mean	95 % BPI
F_v/F_m	0.51	0.49 – 0.52	0.54	0.52 – 0.56
H_a	10.3	5.60 – 19.7	9.04	6.77 – 12.1
H_d	112	85.1 – 142	245	193 – 303
$T_{opt}^{Fv/Fm}$	14.4	12.0 – 16.4	21.1	18.9 – 23.0

F_v/F_m: maximum quantum yield; H_a: activation energy for photosynthesis (kJ mol^{-1}); H_d: deactivation energy (kJ mol^{-1}); $T_{opt}^{Fv/Fm}$: optimum temperature of the maximum quantum yield.

Table 3-3-4. Mean and 95% Bayesian prediction intervals (95% BPI) of parameters estimated from the F_v/F_m–temperature model of *Virescentia helminthosa* and *Sheathia arcuata* from Kagoshima, Japan after 48-h exposure

	Virescentia helminthosa		*Sheathia arcuata*	
Parameter	Mean	95 % BPI	Mean	95 % BPI
F_v/F_m	0.51	0.49 – 0.54	0.55	0.54 – 0.57
H_a	11.0	7.43 – 16.2	8.85	6.64 – 11.8
H_d	219	179 – 263	232	201 – 264
$T_{opt}^{Fv/Fm}$	18.5	16.5 – 20.4	19.2	17.8 – 20.4

F_v/F_m: maximum quantum yield; H_a: activation energy for photosynthesis (kJ mol^{-1}); H_d: deactivation energy (kJ mol^{-1}); $T_{opt}^{Fv/Fm}$: optimum temperature of the maximum quantum yield.

Table 3-3-5. Mean and 95% Bayesian prediction intervals (95% BPI) of parameters estimated from the F_v/F_m–temperature model of *Virescentia helminthosa* and *Sheathia arcuata* from Kagoshima, Japan after 72-hour exposure.

	Virescentia helminthosa		*Sheathia arcuata*	
Parameter	Mean	95 % BPI	Mean	95 % BPI
F_v/F_m	0.52	0.49 – 0.54	0.56	0.54 – 0.58
H_a	13.5	9.57 – 18.9	10.2	8.06– 12.9
H_d	275	229 – 326	339	293 – 386
$T_{opt}^{Fv/Fm}$	18.5	17.1 – 19.7	20.9	19.8 – 21.9

F_v/F_m: maximum quantum yield; H_a: activation energy for photosynthesis (kJ mol^{-1}); H_d: deactivation energy (kJ mol^{-1}); $T_{opt}^{Fv/Fm}$: optimum temperature of the maximum quantum yield.

3.3.5. Combined effects of irradiance and temperature on quantum yields

Responses of the Φ_{PSII} over 12 hours of continuous exposure to 100 (low irradiance) and 1,000 (high irradiance) µmol photons m^{-2} s^{-1} at 12°C, 16°C and 24°C, and their recovery of F_v/F_m after 12-hour dark acclimation are shown in Figs 3-3-4 and 3-3-5.

For *V. helminthosa*, the initial values of F_v/F_m at each irradiance – temperature treatment were 0.492±0.006 SD (16°C, 100 µmol photons m^{-2} s^{-1}) – 0.533±0.006 SD (24°C, 1,000 µmol photons m^{-2} s^{-1}; Fig. 4).The values of Φ_{PSII} of under low irradiance (100 µmol photons m^{-2} s^{-1}) mostly remained stable near the initial value over the 12-h exposure at all three temperature treatments, Φ_{PSII} was 0.474 ± 0.003 SD at 12°C (P < 0.001, Recovery rate from the initial: 93.0%), 0.492 ± 0.010 SD at 16°C (P = 0.935, 100.1%) and 0.469 ± 0.010 SD at 24°C (P < 0.001, 90.0%). Likewise, F_v/F_m subsequent 12-h of dim-light acclimation at each temperature

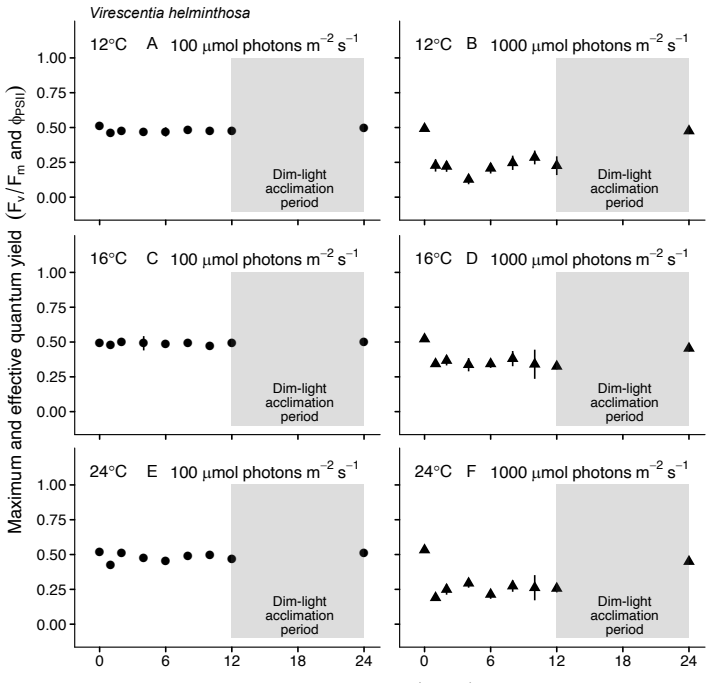

Fig 3-3-4. Hourly response of effective quantum yield (Φ_{PSII}) of *Virescentia helminthosa* to irradiance at 100 (**A, C, E**) and 1,000 µmol photons m^{-2} s^{-1} (**B, D, F**) at 12°C (**A, B**), 16°C (**C, D**) and 24°C (**E, F**). Symbols indicate average of actual values measured (n = 10), and bars indicate standard deviation. Initial values and values after overnight dim-light acclimation (12 h) were measured as maximum quantum yields (F_v/F_m).

was identical with those of the initial value (12°C: 0.499 ± 0.016 SD, $P < 0.1$, 98.0%; 16°C: 0.503 ± 0.015 SD, $P < 0.1$, 102.5%; and 24°C: 0.512 ± 0.008 SD, $P = 0.147$; 98.3%; Fig. 3-3-4). In contrast, the Φ_{PSII} under high irradiance (1,000 μmol photons m^{-2} s^{-1}) over the 12-h exposure at three temperature treatments significantly declined from initial F_v/F_m to Φ_{PSII} of 0.226 ± 0.067 SD at 12°C ($P < 0.001$; 45.9%), 0.325 ± 0.022 SD at 16°C ($P < 0.001$; 62.3%) and of 0.257 ± 0.029 SD at 24°C ($P < 0.001$; 48.2%). The value of F_v/F_m did not fully recover to the initial value subsequent 12-h of dim-light acclimation at 16°C (0.454 ± 0.023 SD, $P < 0.001$; 87.1%) and 24°C (0.450 ± 0.020 SD, $P < 0.001$; 84.4%), respectively. However, it was recovered to the initial value at 12°C (0.475 ± 0.023 SD, $P = 0.37$; 96.6%).

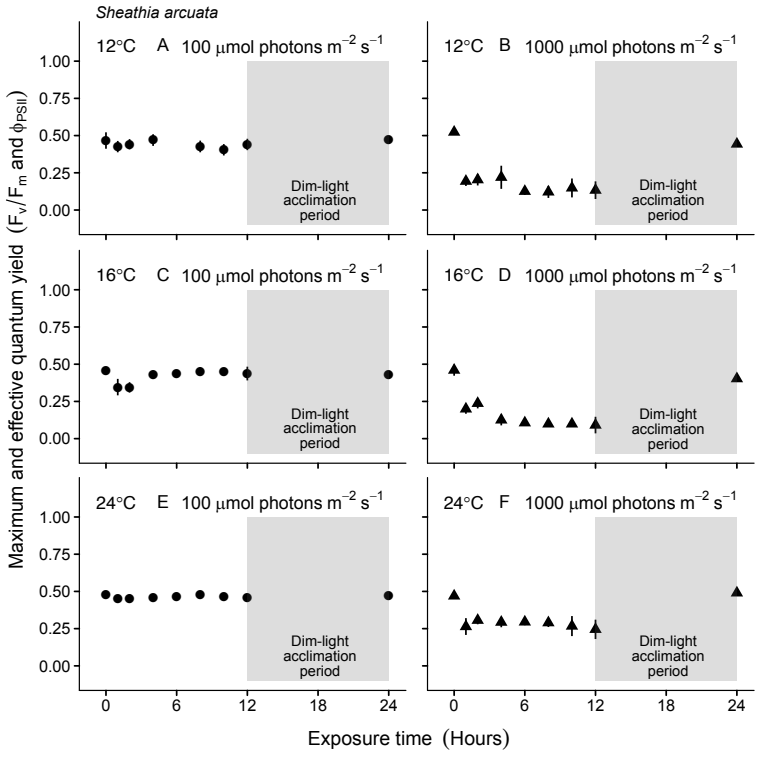

Fig 3-3-5. Hourly response of effective quantum yield (Φ_{PSII}) of *Sheathia arcuata* to irradiance at 100 (**A, C, E**) and 1,000 μmol photons m^{-2} s^{-1} (**B, D, F**) at 12°C (**A, B**), 16°C (**C, D**) and 24°C (**E, F**). Symbols indicate average of actual values measured ($n = 10$), and bars indicate standard deviation. Initial values and values after overnight dim-light acclimation (12 h) were measured as maximum quantum yields (F_v/F_m). The value of Φ_{PSII} in 6-h exposure under 100 μmol photons m^{-2} s^{-1} at 12°C were excluded from the results due the failure of measurement including the inappropriate setting of the equipment.

For *S. arcuata*, the initial values of F_v/F_m at each

irradiance – temperature treatment were 0.458±0.024 SD (16°C, 100 μmol photons m^{-2} s^{-1}) – 0.523±0.015 SD (12°C, 1,000 μmol photons m^{-2} s^{-1}; Fig. 3-3-5). The values of Φ_{PSII} of under low irradiance (100 μmol photons m^{-2} s^{-1}) remained to stable near the initial value over the 12-h exposure at all three temperature treatments, Φ_{PSII} was 0.440 ± 0.038 SD at 12°C (P = 0.145, 94.3%), 0.440 ± 0.046 SD at 16°C (P = 0.153, 95.5%) and 0.456 ± 0.013 SD at 24°C (P < 0.001, 95.0%). Likewise, F_v/F_m subsequent 12-h of dim-light acclimation at each temperature was identical with those of the initial value (12°C: 0.475 ± 0.012 SD, P = 0.641, 101.8%; 16°C: 0.429 ± 0.014 SD, P < 0.1, 93.7%; and 24°C: 0.475 ± 0.007 SD, P = 0.419; 99.0%; Fig. 3-3-5). In contrast, the Φ_{PSII} under high irradiance (1,000 μmol photons m^{-2} s^{-1}) over the 12-h exposure at three temperature treatments significantly declined from initial F_v/F_m to Φ_{PSII} of 0.133 ± 0.059 SD at 12°C (P < 0.001; 25.5%), 0.091 ± 0.056 SD at 16°C (P < 0.001; 19.9%) and of 0.245 ± 0.065 SD at 24°C (P < 0.001; 52.2%). The value of F_v/F_m did not fully recover to the initial value after 12-h of dim-light acclimation at 12°C (0.443 ± 0.019 SD, P < 0.001; 84.7%) and 16°C (0.403 ± 0.012 SD, P < 0.01; 87.5%); however, those at 24°C (0.490 ± 0.011 SD, P = 0.253; 104.4%) were recovered to the initial value.

4. Discussion

Riparian vegetation bordering a reach of a stream or river plays an important role in influencing light and temperature by creating shade (Seath and Hampbrook 1990; Kaczmarczyk and Seath 1991; Giller and Malmqvist 1998; Fujimoto *et al*. 2014; Seath and Vis 2015). In general, habitat of the freshwater red algae varies depending on the species; nevertheless, many species are commonly found under the shaded environment (Kumano 2002; Necchi 2005), suggesting that it might be a strategy to occupy a stable habitat without the competitors. However, in the present study of *T. okadae* that was observed on shallow riverbeds (30–80 cm deep) under the direct sun light, the hourly averaged *in situ* irradiance at noon time in the habitat during winter (December / January) and summer (August) was estimated to be between 153 and 707 μmol photons m^{-2} s^{-1} and 1,205 and 1,311 μmol photons m^{-2} s^{-1}, respectively. The daily integrated *in situ* irradiance during the two seasons ranged between 6,447 and 16,019 mmol photons m^{-2} d^{-1} and 24,711 and 34,616 mmol photons m^{-2} d^{-1}, respectively, suggesting that *in situ* irradiance environment in the habitats of *T. okadae* was 30~50 times higher than those of *T. gaudichaudii* in the present study and Terada *et al.* (2016).

In the heteromorphic life history of *T. okadae*, the microscopic life history stage (sporophyte; known as *Chantransia*-phase) was reported to persist year-round; whereas,

the macroscopic life history stage (gametophyte) occurs only in winter including early winter and late spring (Higa *et al.* 2007). Based on a few days of measurement with the quantum loggers that included sunny days without clouds in the sky, the maximum *in situ* irradiance at the habitat was observed to be up to 868 μmol photons m^{-2} s^{-1} during the noon time in winter (December / January) when the macroscopic life history stage was observed. Furthermore, in summer (August), the maximum *in situ* irradiance at the habitat was up to 1,392 μmol photons m^{-2} s^{-1}, indicating that *T. okadae* is potentially exposed to relatively high irradiance, in contrast to *N. tortuosa* and *T. gaudichaudii* (Fujimoto *et al.* 2014; Terada *et al.* 2016). Since, the microscopic life history stage of *T. okadae* can occur abundantly during the summer (August and September), this microscopic stage is likely exposed to relatively high irradiance (Higa *et al.* 2007). Our study, has confirmed the occurrence of the microscopic stage on pebbles and cobbles in the riverbed under direct sun light.

In contrast, the hourly averaged incident irradiance at midday in the habitat of *T. gaudichaudii* from Yoron-jima island, Kagoshima Prefecture, Japan was reported to be between 5.6 and 18.6 μmol photons m^{-2} s^{-1} (Terada *et al*. 2016c), suggesting that *T. gaudichaudii* is believed to be adapted to the heavily shaded environment. This spring in Yoron-jima where *T. gaudichaudii* grows is covered by an artificial concrete-made roof

(Terada *et al*. 2016c); on the one hand, a habitat of "*Ufukubuga*" in Okinawa-jima island in the present study had no artificial roof over the spring, suggesting the possibility of occurrence of direct sunlight on this habitat. Nevertheless, incident irradiance on the thallus at midday was less than 100 μmol photons m^{-2} s^{-1} due to the shading by a basin wall, nearby vegetation and an embankment that surrounded the study site. The area was mostly shaded from direct light, but there we short instances of direct sunlight through a gap in the trees in the late afternoon. At this moment, irradiance reached instantly around 300 μmol photons m^{-2} s^{-1}; however, the exposure time of direct sunlight was quite limited, suggesting that the habitat was predominantly under shaded conditions. Despite these shaded conditions, *T. gaudichaudii* exhibited a midday depression of Φ_{PSII} as irradiance peaked at midday, followed by an upturn as irradiance decreased by the late evening.

In the present study, *V. helminthosa* and *S. arcuata* were found in the irrigation canal partly shaded by the surrounding riparian vegetation (60 – 170 μmol photons m^{-2} s^{-1}). Nevertheless, these two species were also patchily found on the canal floor with no shade where the irradiance under the noontime reaches 1,600 μmol photons m^{-2} s^{-1}, suggesting that *in situ* light environment for two species seems to vary from 60 – 1600 μmol photons m^{-2} s^{-1} depending of the amount of riparian vegetation. Indeed, oxygenic *P–E* curves for *V. helminthosa* and *S. arcuata* showed similar irradiance responses, and

quickly saturated with the relatively low values of E_c (6.95 [5.58–8.42, BPI] and 11.5 [9.10–14.2, BPI] μmol photons m^{-2} s^{-1}, respectively) and E_k (18.8 [14.5–24.7, BPI] and 17.7 [13.0–23.9, BPI] μmol photons m^{-2} s^{-1}, respectively), revealing the low irradiance adaptation in the oxygenic photosynthesis that enables the occurrence of these algae under the shaded environment.

Likewise, reduction in oxygenic evolution was observed in two life-history stages of *T. gaudichaudii* up to 1,000 μmol photons m^{-2} s^{-1}, and it was more pronounced in the microscopic stage. Results of the oxygenic *P–E* curve of *T. gaudichaudii* indicated that E_c and E_k in two life-history stages (6.71 and 26.6 μmol photons m^{-2} s^{-1} for macroscopic stage; 2.56 and 30.0 μmol photons m^{-2} s^{-1} for microscopic stage, respectively) were similar to each other, and were closely related to the results of *V. helminthosa* and *S. arcuata* in the present study and to the previous study of macroscopic stage of *T. gaudichaudii* (7 and 12 μmol photons m^{-2} s^{-1}; Terada *et al*. 2016c) and macroscopic thalli of *N. tortuosa* (8 and 10 μmol photons m^{-2} s^{-1}; Fujimoto *et al*. 2014). In fact, adaptation to a low irradiance environment was widely reported from many freshwater red algae from Brazil including *Compsopogon* (Compsopogonales), *Sirodotia* (as *Batrachospermum*, Batrachospermales) and *Thorea* (Necchi and Zucchi 2001; Necchi 2005; Kusakariba and Necchi 2009). However, unlike the results of *T. gaudichaudii*,

characteristic photoinhibition was less pronounced in their *P–E* curves of *V. helminthosa* and *S. arcuata* under the irradiance of 500 and 1,000 μmol photons m^{-2} s^{-1}.

In contrast, the oxygenic *P–E* curve of *T. okadae* indicated that E_k (55.2 [42.2–72.9, BPI] μmol photons m^{-2} s^{-1}) was relatively higher than those of *V. helminthosa*, *S. arcuata* and *T. gaudichaudii* in the present study and those of *N. tortuosa* (10 μmol photons m^{-2} s^{-1}; Fujimoto *et al.* 2014). Therefore, like *Sirodotia delicatula* Sukuja (as *Batrachospermum delicatulum* (Skuja) Necchi et Entwisle) from Brazil that can be adapted to the high irradiance (E_k = 204 μmol photons m^{-2} s^{-1} ± 34.8 SD, Necchi 2005), *T. okadae* is likely to actively undergo photosynthesis under conditions of relatively high irradiance.

Nevertheless, oxygenic photoinhibition was observed in the *P–E* curve of *T. okadae* at irradiance of 1,000 μmol photons m^{-2} s^{-1}, which suggests that irradiance during midday with clear skies in winter is close to inhibitory. Indeed, Φ_{PSII} of the photosynthetic efficiency in *PSII* of *T. okadae* significantly declined during continuous exposure to 1,000 μmol photons m^{-2} s^{-1} at both 12°C and 24°C, and F_v/F_m showed failure to recover in post-dark acclimation. Similar chronic depression of Φ_{PSII} during high light exposure at 1,000 μmol photons m^{-2} s^{-1} was also observed in *V. helminthosa*, *S. arcuata* and *T. gaudichaudii* in the present study. Chronic photoinhibition occurs when the rate of degradation exceeds

that of the repair system of *PSII* (Aro *et al*. 2005; Nishiyama *et al*. 2006; Takahashi and Badger 2011). The failure of recovery in post-dark acclimation F_v/F_m in the present study may also be related to the increased rate of degradation or damage to *PSII,* which remains to be investigated.

Nevertheless, Φ_{PSII} of *PSII* at 22°C and 24°C under low irradiance (50 or 100 μmol photons m^{-2} s^{-1}) for four species seemed steady during exposure with a full recovery of F_v/F_m after 12-h dark or dim-light acclimation. However, under low irradiance at 12°C, F_v/F_m of *T. gaudichaudii* more depressed than at 22°C, suggesting low temperature-induced the photoinhibition (Borlongan *et al.* 2018; Terada *et al*. 2018, 2019; Fukumoto *et al*. 2018, 2019). Failure of F_v/F_m to recover was also more pronounced under high irradiance and low temperature in *T. okadae* (67.7%; at 12°C and 1,000 μmol photons m^{-2} s^{-1}), and implies that inhibitory effects were accelerated by the combined effect of low temperature and high light that is similar to chilling-light stress (Borlongan *et al.* 2017, 2018; Terada *et al.* 2018; Fukumoto *et al.* 2018). Low temperatures altered the repair of *PSII*, including their *de novo* synthesis of D_1 protein repair system, given that protein synthesis decreases with declining temperatures (Allakhverdiev and Murata 2004; Takahashi and Murata 2008), and seem to prevent the full recovery of the algae from photoinhibition. However, based on the diurnal fluctuation of *in situ* irradiance in the

habitat, we note that such inhibitory high irradiance is limited only around midday under fine clear skies. Hence, occurrence of chilling-light stress of four species would be rare at the study sites. However, we noted in winter that relatively excessive irradiance might induce photoinhibition.

More interestingly, chronic depression of Φ_{PSII} under 1,000 μmol photons m^{-2} s^{-1} (high irradiance) for *V. helminthosa* and *S. arcuata* revealed that their F_v/F_m of the *PSII* was mostly recovered after a subsequent 12-h dim-light acclimation, suggesting the potential of recovery of *PSII* photochemical efficiency from the daytime chronic photoinhibition. Nevertheless, these results of the chronic light exposure and acclimation in the present study need to be interpreted with caution in comparison with the results of *T. okadae* and *T. gaudichaudii*, as a more typical failure of recovery may have occurred if the subsequent acclimation was done in complete darkness (0 μmol photons m^{-2} s^{-1}). Indeed, the use of dim-light conditions (10–30 μmol photons m^{-2} s^{-1}) has been better for complete recovery than those of complete darkness (0 μmol photons m^{-2} s^{-1}), since dim light is essential for the activation of D_1 synthesis. Furthermore, the diurnal change of Φ_{PSII} values in *S. delicatula* was reported to be negatively correlated with incident irradiance under the natural state (Kusakariba and Necchi 2009). Their data also revealed high excitement pressure on *PSII* and good recovery capacity and a lack of irreversible

photodamage to photosynthetic apparatus due to the prolonged exposure to high irradiance (Kusakariba and Necchi 2009).

The optimum temperature (T_{opt}^{GP}) for the oxygenic maximum gross photosynthesis (GP_{max}) in *T. okadae*, *V. helminthosa* and *S. arcuata* was 30.8°C, (30.0–31.7, BPI), 26.4°C (23.9–28.7, BPI) and 30.3°C (28.3–32.1, BPI), respectively, and was well above temperatures observed during its occurrence at the study sites and those of a previous study (9–18°C, Fujimoto *et al.* 2014). Furthermore, those of macroscopic and microscopic stages of *T. gaudichaudii* (32.1°C [29.8–34.0, BPI] and 35.7°C [29.5–48.6, BPI]) were also well above temperatures observed during its occurrence at the study site (23°C). In fact, temperature optima of oxygenic photosynthesis have been generally known to be well above the temperature optima for growth (Davison 1987; Eggert and Wiencke 2000; Eggert 2012). Such disparity is common as growth involves an integration of all metabolic processes, including photosynthesis (Eggert and Wiencke 2000; Eggert 2012). Although considered as the optimum temperature (T_{opt}^{GP}), this should be regarded as where the macrophyte is close to a physiologically critical state including the enzyme deactivation and photodamage (Terada *et al*. 2016a, b, c, 2018, 2019).

Unlike temperature optima (T_{opt}^{GP}) for the oxygenic photosynthesis, modeled optimum temperature for the F_v/F_m of *PSII* ($T_{opt}^{Fv/Fm}$) for *T. okadae*, two life-history stages

of *T. gaudichaudii*, *V. helminthosa* and *S. arcuata* was 18.4°C (17.0 – 19.8, BPI), 17.8°C (16.7 – 18.8, BPI), 15.0°C (12.3 – 17.1), 18.5°C (17.1 – 19.7, BPI) and 20.9°C (19.8 – 21.9, BPI; $T_{opt}^{Fv/Fm}$), respectively, and was almost consistent with the water temperature of their occurrence period in the habitat, but quickly declined at much higher temperatures. The decline of F_v/F_m (based on the equation, $F_v/F_m = (F_m - F_o) / F_m$) from thermal stress may be attributable to increase in minimum fluorescence (F_o) and decrease in maximum fluorescence (F_m). This is expected based on reductions in the primary and secondary quinone electron acceptors (Q_A and Q_B) in the *PSII* reaction center (RCII; Pospíšil *et al.* 1998). The *PSII* deactivation that was observed may also be due to thermal stress, related to structural rearrangements in the thylakoid membranes (Roleda 2009; Hanelt and Figueroa 2012; Beer *et al*. 2014), or to accumulation of hydrogen peroxide that inhibits *de novo* synthesis of D_1 protein in *PSII* (Allakhverdiev and Murata 2004; Allakhverdiev *et al*. 2008; Takahashi and Murata 2008). Furthermore, relatively long-hour temperature exposure up to 72 hours for *V. helminthosa* and *S. arcuata* might also negatively influence all metabolic processes in the algal thallus especially at high temperatures, and enhanced the thermal decline of the F_v/F_m of *PSII*.

More interestingly, in *T. gaudichaudii*, optimum temperature of oxygenic photosynthesis (T_{opt}^{GP}) and those of the maximum F_v/F_m ($T_{opt}^{Fv/Fm}$) in the two life-history

stages were also similar between stages. In the heteromorphic life history of marine algae, temperature optima of two life-history stages are also known to differ. In the red algae, *P. tenera* and *P. yezoensis*, this difference was also regarded as an adaptation to environmental conditions during the different occurrence period of each generation (Bessho and Iwasa 2009, 2010, 2012; Watanabe *et al.* 2014; 2016). In contrast, those with similar optima occurred in the algae of Ectocarpales and Laminariales (Phaeophyceae; Fukumoto *et al*. 2018, 2019; Borlongan *et al*. 2018, 2019). This similarity of temperature optima suggests a possibility that there is overlap in the occurrence of the two life-history stages in the natural habitat (Borlongan *et al*. 2018; Fukumoto *et al.* 2018). In the present study, the two life-history stages of *T. gaudichaudii* is known to persist year-round under the less seasonal fluctuation of water temperature from the spring (Terada *et al*. 2016c; Higa 2018); therefore, the similar temperature optima might result from the overlap in the occurrence of the two life-history stages.

Furthermore, as Migita and Toma (1990) reported that the macroscopic stage of this alga has both asexual and sexual reproductions on the thallus, asexual reproduction and monospore release from the macroscopic stage was observed at temperatures between 15 to 25°C, which grew into the macroscopic erect thalli via the *Chantransia*-stage. In contrast, sexual organs such as spermatangia and carposporangia were produced on the

macroscopic thallus only at warm temperatures of 25°C, suggesting that the life cycle of this alga at the study site where the water temperature never reaches above 24°C may have mainly occurred through asexual reproduction between macroscopic and microscopic (*Chantransia*) stages without meiosis (Terada *et al.* 2016c). If so, the *Chantransia*-stage at the study site may be regarded as part of the haploid-phase, together with the macroscopic stage during their life cycle, and the similarity in temperature and irradiance optima among the two stages is may be linked to similarity in nuclear phase. However, knowledge for the *in vitro* growth of the carpospore and the possibility of the occurrence of *Chantransia*-stage form from carpospores has not been elucidated for this species. Further studies to confirm the presence of meiosis and diploid/haploid-phase in the microscopic-stage are essential for the future (see: Remarks of page 86 in Necchi 2016).

Given the results of the four freshwater red algae can be regarded to be well adapted to a low irradiance environment but can also be a partly tolerable relatively high irradiance environment that enables them to occur on the canal floor with no shade. Chronic exposure to irradiance at magnitudes at 1,000 μmol photons m^{-2} s^{-1} is likely to lead to chronic photoinhibition; however, declined *PSII* photochemical efficiency can be recovered during subsequent night-time acclimation including dim light environment at

evening and morning twilight. Nevertheless, shading by the surrounding riparian vegetation is beneficial for many freshwater algae including these two species (Fujimoto *et al.* 2014; Terada *et al.* 2016c), and it is relevant when proposing strategies for conservation and restoration. Finally, other biotic and/or abiotic factors, including water velocity, flooding frequency, nutrient availability, specific conductivity, and competitors, may also influence the abundance and occurrence of this species and should be studied in the future.

Acknowledgements

I express my gratitude to Prof. Ryuta Terada, Vice-Dean of The United Graduate School of Agricultural Sciences (UGSAS), Kagoshima University, and Dr. Gregory N. Nishihara, Institute for East China Sea Research, Organization for Marine Science and Technology, Nagasaki University, for their untiring support and encouragement during the study in MSc and PhD programs. I also thank Prof. Tomoko Yamamoto, Dr. Hikaru Endo, Faculty of Fisheries, Kagoshima University, Prof. Hiroyuki Motomura, Kagoshima University Museum, and Dr. Kei Kimura, Faculty of Agriculture, Saga University, for their constructive comments and support during my study and the PhD dissertation committee. Cordial thank is due to Mr. Kazuo Nirei, Yoron Municipal Office, and Mr. Atsushi Higa,

Okinawa Environmental Analysis Center, Co. Ltd., for their kind arrangements and suggestions of the field survey. Finally, I am grateful to Dr. Masafumi Iima, Faculty of Environmental Science, Nagasaki University who introduced me to the world of algae at my undergraduate student days.

References

Agardh CA (1824) Systema Algarum. Lundae, Literis Berlingianis

Alexandrov GA, Yamagata Y (2007) A peaked function for modeling temperature dependence of plant productivity. Ecol Model 200: 189–192

Allakhverdiev SI, Kreslavski VD, Klimov VV, Los DA, Carpentier R, Mohanty P (2008) Heat stress: an overview of molecular responses in photosynthesis. Photosynth Res 98: 541–550

Allakhverdiev SI, Murata N (2004) Environmental stress inhibits the synthesis *de novo* of proteins involved in the photodamage-repair cycle of photosystem II in *Synechocystis* sp. PCC 6803. Biochim Biophys Acta 1657: 23–32

Aro EM, McCaffery S, Anderson JM (1994) Recovery of photoinhibition in Peas (*Pisum sativum* L.) acclimated to varying growth irradiances. Role of D_1 protein turnover. Plant Physiol 104: 1033–1041

Aro EM, Surosa M, Rokka A, Allahverdiyeva Y, Paakkarinen V, Saleem A, Battchikova N, Rintama E (2005) Dynamics of photosystem II: a proteomic approach to thylakoid protein complexes. J Exp Bot 56: 347–356

Beer S, Björk M, Beardall J (2014) Photosynthesis in the marine environment. Wiley-Blackwell, Ames, Iowa

Bellasio C, Burgess SJ, Griffiths H, Hibberd JM (2014) A high throughput gas exchange screen for determining rates of photorespiration or regulation of C_4 activity. J Exp Bot 65: 3769–3779

Bessho K. Iwasa Y (2009) Heteromorphic and isomorphic alternations of generations in macroalgae as adaptations to a seasonal environment. Evol Eco. Res 11: 691–711

Bessho K. Iwasa Y 2010. Optimal seasonal schedules and the relative dominance of heteromorphic and isomorphic life cycles in macroalgae. J Theor Biol 267: 201–212

Bessho K. Iwasa Y 2012. Variability in the evolutionarily stable seasonal timing of germination and maturation of annuals and the mode of competition. J Theor Biol 304: 66–80

Borlongan IA, Nishihara GN, Shimada S, Watanabe Y, Terada R (2017) Effects of temperature and PAR on the photosynthesis of *Kappaphycus* sp. (Soloeriaceae,

Rhodophyta) from Okinawa, Japan, as the northern limited of native *Kappaphycus* distribution in the western Pacific. Phycologia 56: 444–453

Borlongan IA, Matsumoto K, Nakazaki Y, Shimada N, Kozono J, Nishihara GN, Shimada S, Watanabe Y, Terada R (2018) Photosynthetic activity of two life history stages of *Costaria costata* (Laminariales, Phaeophyceae) in response to PAR and temperature gradient. Phycologia 57: 159–168

Borlongan IA, Nishihara GN, Shimada S, Terada R (2019) Assessment of photosynthetic performance in the two life history stages of *Alaria crassifolia* (Laminariales, Phaeophyceae). Phycol Res 67: 28–38

Cosgrove J, Borowitzka MA (2011) Chlorophyll fluorescence terminology: An introduction. In: Suggett DJ, Prásil O, Borowitzka MA (eds) Chlorophyll a fluorescence in aquatic sciences: methods and applications. Springer, Dordrecht, pp 1–17

Davison IR (1987) Adaptation of photosynthesis in *Laminaria saccharina* (Phaeophyta) to changes in growth temperature. J Phycol 23: 273–283

Eggert A (2012) Seaweed responses to temperature. In: Wiencke, C. and Bischof, K. (Eds) Seaweed Biology. Springer, Berlin Heidelberg. pp 47–66

Eggert A, Wiencke C (2000) Adaptation and acclimation of growth and photosynthesis

of five Antarctic red algae to low temperatures. Polar Biol 23: 609–618

Fujimoto M, Nitta K, Nishihara GN, Terada R (2014) Phenology, irradiance and temperature characteristics of a freshwater red alga, *Nemalionopsis tortuosa* (Thoreales), from Kagoshima, southern Japan. Phycol Res 62: 77–85

Fukumoto R, Borlongan IA, Nishihara GN, Endo H, Terada R (2018) The photosynthetic responses to PAR and temperature including chilling-light stress on the heteromorphic life history stages of a brown alga, *Cladosiphon okamuranus* (Chordariaceae) from Ryukyu Islands, Japan. Phycol Res 66: 209–217

Fukumoto R, Borlongan IA, Nishihara GN, Endo H, Terada R (2019) Effect of photosynthetically active radiation and temperature on the photosynthesis of two heteromorphic life history stages of a temperate edible brown alga, *Cladosiphon umezaki*i (Chordariaceae, Ectocarpales), from Japan. J Appl Phycol 31: 1259–1270.

Gelman A (2004) Parameterization and Bayesian Modeling. J Am Stat Assoc 99: 537–545

Gelman A (2006) Prior distributions for variance parameters in hierarchical models. Bayesian Anal 1: 515–533

Giller PS, Malmqvist B (1998) The biology of streams and rivers. Oxford University Press, Oxford

Hanelt D, Figueroa FL (2012) Physiological and photomorphogenic effects of light on marine macrophytes. In: Wiencke C, Bischof K (eds) Seaweed Biology, Springer, Berlin, Heidelberg, pp. 3–23

Hanelt D, Melchersmann B, Wiencke C, Nultsch W (1997) Effects of high light stress on photosynthesis of polar macroalgae in relation to depth distribution. Mar Ecol Prog Ser 149: 255–266

Hanelt D, Wiencke C, Karsten U, Nultsch W (1997) Photoinhibition and recovery after high light stress in different developmental and life-history stages of *Laminaria saccharina* (Phaeophyta). J Phycol 33: 387–395

Henley WJ (1993) Measurement and interpretation of photosynthetic light-response curves in algae in the context of photoinhibition and diel changes. J Phycol 29: 729–739

Higa A, Kasai F, Kawachi M, Kumano S, Sakayama H, Miyashita M, Watanabe MM (2007) Seasonality of gametophyte occurrence, maturation and fertilization of the freshwater red alga, *Thorea okadae* (Thoreales, Rhodophyta) in the Kikuchi River, Japan. Phycologia 46: 160-167

Higa A (2018) *Thorea gaudichaudii.* In: Okinawa Prefecture (ed) Threatened Wildlife in Okinawa. Red Data Okinawa third ed. (Fungi and Plants). Department of

Environmental Affairs, Okinawa Prefectural Government, Naha, pp. 579–580 (in Japanese)

Japanese Ministry of Environment (2019) Red List, 4th edition, revised in 2019. http://www.env.go.jp/press/106383.html (Accessed 10 August 2019; in Japanese)

Jassby AD, Platt T (1976) Mathematical formulation of the relationship between photosynthesis and light for phytoplankton. Limnol Oceanogr 21: 540–547

Kaczmarczyk D, Seath RG (1991) The effect of light regime on the photosynthetic apparatus of the freshwater red alga *Batrachospermum boryanum*. Cryptogamie Algol 12: 249–263

Kokubu S, Nishihara GN, Watanabe Y, Tsuchiya Y, Amano Y, Terada R (2015) The effect of irradiance and temperature on the photosynthesis of a native brown alga, *Sargassum fusiforme* (Fucales) from Kagoshima, Japan. Phycologia 54: 235–247

Kumano S (2002) Freshwater Red Algae of the World. Biopress Limited, Bristol

Kusakariba T, Necchi O Jr (2009) Daily dynamics of photosynthesis of the freshwater red alga *Sirodotia delicatula* (Batrachospermales, Rhodophyta). Phycol Res 57: 268–277

Migita S, Toma T (1990) Culture studies of freshwater red alga *Thorea gaudichaudii* (Rhodophyta, Nemaliales). Bull Fac Fish Nagasaki Univ 68: 7–12 (in Japanese)

Necchi O Jr (1987) Sexual reproduction in *Thorea* BORY (Rhodophyta, Thoreaceae). Jpn J Phycol 35: 106–112

Necchi O Jr (2005) Light-related photosynthetic characteristics of freshwater Rhodophyta. Aqua Bot 82: 193–209

Necchi O Jr. (2016) Ecophysiology of river algae. In: Necchi O Jr (ed) River algae. Springer, Cham, Switzerland, pp. 65–91

Necchi O Jr, Zucchi MR (2001) Photosynthetic performance of freshwater Rhodophyta in response to temperature, irradiance, pH and diurnal rhythm. Phycol Res 49: 305–318

Nishiyama Y, Allakhverdiev S, Murata N (2006) A new paradigm for the action of reactive oxygen species in the photoinhibition of photosystem II. Biochim Biophys Acta 1757: 742–749

Platt T, Gallegos CL, Harrison WG (1980) Photoinhibition of photosynthesis in natural assemblages of marine phytoplankton. J Mar Res 38: 687–701

R Development Core Team (2018) R: A language and environment for statistical computing. R Foundation for Statistical Computing, Vienna, Austria. ISBN 3-900051-07-0, URL http://www.R-project.org (Accessed 10 August 2018).

Roleda MY (2009) Photosynthetic response of Arctic kelp zoospores exposed to radiation

and thermal stress. Photochem Photobiol Sci 8: 1302–1312

Sabater S, Artigas J, Corcoll N, Proia L, Timoner X, Tornés E (2016) Ecophysiology of river algae. In: Necchi O Jr (ed) River algae. Springer, Cham, Switzerland, pp. 197–217

Sato H, Sugino N, Nagano M, Yonei S, Fujimoto T, Higashiyama M (2013) Life history stages and seasonality of a freshwater red alga Thorea okadae Yamada (Thoreales, Rhodophyta) in the Yasumuro River, Kamigori, Hyogo Prefecture, Japan. Jpn J. Phycol 61: 1–5 (in Japanese with English abstract)

Schubert N, Colombo-Pallota MF, Enríquez S (2015) Leaf and canopy scale characterization of the photoprotective response to high-light stress of the seagrass *Thalassia testudinum*. Limnol Oceanogr 60: 286–302

Seath RG, Hampbrook JA (1990) Freshwater ecology. In: Cole KM, Sheath RG (eds) Biology of the red algae. Cambridge University Press, Cambridge, pp. 423–453

Seath RG, Vis ML (2015) Red algae. In: Wehr JD, Seath RG, Kociolek JP (eds) Freshwater algae of North America, Ecology and classification, second edition. Academic Press, London, pp. 237–264

Seto R (1979) Comparative study of *Thorea gaudichaudii* (Rhodophyta) from Guam and Okinawa. Micronesica 15: 35–9

Seto R, Migita S, Madono K, Kumano S (1993) A freshwater red alga, *Thorea okadai* Yamada from Yasumuro-River in Hyogo Prefecture and geographical distribution of the species of *Thorea* in Japan. Jpn J. Phycol 41: 355–357 (in Japanese)

Stan Development Team (2018) Stan: A C++ Library for Probability and Sampling, Version 2.14.2. URL http://mc-stan.org (Accessed 10 August 2018)

Suzawa T, Suzawa Y, Nakajima J, Take M (2010) First record of *Thorea gaudichaudii* C. Agardh from Yoron Island, Kagoshima Prefecture. Jpn. J. Phycol. 58: 141–143 (in Japanese)

Takahashi S, Badger M (2011) Photoprotection in plants: a new light on photosystem II damage. Trends in Plant Science 16: 53–60

Takahashi S, Murata N (2008) How do environmental stresses accelerate photoinhibition? Trends Plant Sci 13: 178–182

Tcherkez G, Bligny R, Gout E, Mahé A, Hodges M, Cornic G (2008) Respiratory metabolism of illuminated leaves depends on CO_2 and O_2 conditions. Proc Natl Acad Sci USA 105: 797–802

Terada R (2015a) *Thorea gaudichaudii*. In: Japanese Ministry of Environment (ed) Red Data Book 2014, Threatened Wildlife of Japan, Volume 9, Bryophytes, Algae, Lichens, Fungi. Gyosei Cooperation, Tokyo, pp. 295 (in Japanese)

Terada R (2015b) *Thorea okadae*. In: Japanese Ministry of Environment (ed) Red Data Book 2014, Threatened Wildlife of Japan, Volume 9, Bryophytes, Algae, Lichens, Fungi. Gyosei Cooperation, Tokyo, pp. 369. Tokyo. (in Japanese)

Terada R, Matsumoto K, Borlongan IA, Watanabe Y, Nishihara GN, Endo H, Shimada S (2018) The combined effects of PAR and temperature including the chilling-light stress on the photosynthesis of a temperate brown alga, *Sargassum patens* (Fucales), based on field and laboratory measurements. J Appl Phycol 61: 1893–1904

Terada R, Nakashima Y, Borlongan IA, Shimabukuro H, Kozono J, Endo H, Shimada S, Nishihara GN (2019) Photosynthetic activity including the thermal- and chilling-light sensitivities of a temperate Japanese brown alga *Sargassum macrocarpum*. Phycol Res DOI: 10.1111/pre.12398 (Online)

Terada R, Vo TD, Nishihara GN, Matsumoto K, Kokubu S, Watanabe Y, Kawaguchi S (2016a) The effect of PAR and temperature on the photosynthesis of two Vietnamese species of *Sargassum*, *Sargassum mcclurei* and *Sargassum oligocystum*, based on the field and laboratory measurements. Phycol Res 64: 230–40

Terada R, Vo DT, Nishihara GN, Shioya K, Shimada S, Kawaguchi S (2016b) The effect of irradiance and temperature on the photosynthesis and growth of a cultivated red

alga *Kappaphycus alvarezii* (Solieriaceae) from Vietnam, based on in situ and in vitro measurements. J Appl Phycol. 28: 457–67

Terada R, Watanabe Y, Fujimoto M, Tatamidani I, Kokubu S, Nishihara GN (2016c) The effect of PAR and temperature on the photosynthetic performance of a freshwater red alga, *Thorea gaudichaudii* (Thoreales) from Kagoshima, Japan. J Appl Phycol 28: 1255–1263

Thornley JHM, Johnson IR (2000) Plant and Crop Modelling: A mathematical approach to plant and crop physiology. Blackburn Press, Caldwell, New Jersey

Watanabe Y, Nishihara GN, Tokunaga S, Terada R (2014) The effect of irradiance and temperature on the photosynthesis of a cultivated red alga, *Pyropia tenera* (= *Porphyra tenera*), at the southern limit of distribution in Japan. Phycol. Res. 62: 187–96

Watanabe Y, Yamada H, Mine T, Kawamura Y, Nishihara GN, Terada R (2016) Photosynthetic responses of *Pyropia yezoensis* f. *narawaensis* (Bangiales, Rhodophyta) to a thermal and PAR gradient vary with the life-history stage. Phycologia 55: 665–72

Webb WL, Newton M, Starr D (1974) Carbon dioxide exchange of *Alnus rubra*: a mathematical model. Oecologia 17: 281–291

Yamada Y (1949) On the species of *Thorea* from the far eastern Asia. Jpn J Bot 24: 155–159

Yoshizaki M (1993) The morphology and reproduction of *Thorea okadai* (Rhodophyta). Phycologia 25: 476–481